

1 **The SLC25 carrier family: important transport proteins in mitochondrial**  
2 **physiology and pathology**

3 Edmund R.S. Kunji<sup>1\*</sup>, Martin S. King<sup>1</sup>, Jonathan J. Ruprecht<sup>1</sup>, Chancievan Thangaratnarajah<sup>2</sup>

4  
5 **Orcid numbers**

6 CT, 0000-0002-0279-6642; MSK, 0000-0001-6030-5154; JJR, 0000-0002-1838-7245; ERSK  
7 0000-0002-0610-4500

8  
9 **Affiliation**

10 <sup>1</sup>Medical Research Council Mitochondrial Biology Unit, University of Cambridge, Cambridge  
11 Biomedical Campus, Keith Peters Building, Hills Road, Cambridge, CB2 0XY, United Kingdom

12 <sup>2</sup>University of Groningen, Groningen Biomolecular Sciences and Biotechnology Institute,  
13 Membrane Enzymology, Nijenborgh 4, 9747 AG Groningen, The Netherlands

14  
15 **Running head** Disease variants of mitochondrial carriers

16  
17 **Address for correspondence**

18 \*Edmund R.S. Kunji, Medical Research Council Mitochondrial Biology Unit, University of  
19 Cambridge, Cambridge Biomedical Campus, Keith Peters Building, Hills Road, Cambridge,  
20 CB2 0XY, United Kingdom. Telephone +44-1223-252850, ek@mrc-mbu.cam.ac.uk

21  
22 **Abstract**

23 Members of the mitochondrial carrier family (SLC25) transport a variety of compounds  
24 across the inner membrane of mitochondria. These transport steps provide building blocks  
25 for the cell and link the pathways of the mitochondrial matrix and cytosol. An increasing  
26 number of diseases and pathologies has been associated with their dysfunction. In this  
27 review, the molecular basis of these diseases is explained based on our current  
28 understanding of their transport mechanism.

29  
30 **Keywords** mitochondrial physiology, mitochondrial disease, impaired transport mechanism,  
31 pathological mutations, bioenergetics

32

### 33 **Introduction**

34 The inner membrane of mitochondria is highly impermeable to molecules and ions, which is  
35 a key property required for energy conversion in oxidative phosphorylation. Therefore, a  
36 large number of transport proteins and channels are required to transport molecules and  
37 ions across this membrane to link cytosolic and mitochondrial metabolism, and to provide  
38 compounds for building and maintenance of the mitochondrion and the cell. In fact, all  
39 major food groups pass through the mitochondrion as part of central metabolism, including  
40 the degradation products of fats, sugars, and proteins as well as nucleotides, vitamins and  
41 inorganic ions (FIGURE 1). Most of the transport steps are carried out by members of the  
42 mitochondrial carrier family (SLC25), the topic of this review, but there also other  
43 transporter families, such as the mitochondrial pyruvate carrier (SLC54) (19, 61),  
44 sideroflexins (SLC56) (87, 127, 170) and mitochondrial ABC transporters (98, 148).  
45 Mitochondrial carriers provide key transport steps in a variety of metabolic pathways, such  
46 as the oxidation of degradation products of fats and sugars, the degradation, synthesis and  
47 interconversion of amino acids, and the synthesis of iron sulfur clusters and heme, but also  
48 in ion homeostasis, mitochondrial macromolecular synthesis, heat production,  
49 mitochondrial dynamics, signaling, cellular differentiation, development, and cell death (89,  
50 123). The genes of 53 mitochondrial carriers of the SLC25 family have been identified in the  
51 human genome (89, 123), based on their shared sequence features (137, 147) and structural  
52 properties (128, 141, 143, 144). Most carriers are found in the inner membrane of the  
53 mitochondrion, but an adenine nucleotide transporter (SLC25A17) has been located in the  
54 peroxisome, where it supplies ATP for energy-requiring processes (161). Moreover, two  
55 highly divergent carriers, SLC25A46 and SLC25A50 (MTCH2), have been localized to the outer  
56 membrane of the mitochondrion (2, 172), where they might have some involvement in  
57 mitochondrial dynamics and apoptosis, respectively, but no transport function has been  
58 assigned to them.

59 Mitochondrial carriers are functional as monomers (10-12, 32, 91). The only  
60 confirmed exception is the mitochondrial aspartate/glutamate carrier, which is a structural  
61 dimer through the interactions of the N-terminal calcium regulatory domains, but the carrier  
62 domains, which are involved in transport, function separately (see further below) (157).  
63 Recently, a claim was made for the bovine mitochondrial ADP/ATP carrier being monomeric  
64 and dimeric using native mass spectrometry of intact membranes (28), but the reported

65 mass deviates significantly from those observed by others (7, 62, 153). To account for the  
66 difference, the carrier was proposed to have an unusually large number of modifications,  
67 which have not been observed in other studies (7, 153) or in the structure (128).  
68 Furthermore, the species observed by native mass spectrometry lacks three tightly bound  
69 cardiolipin molecules (28), which are observed consistently in other studies (10, 14, 96, 128,  
70 141, 142).

71         Given the central role of mitochondrial carriers in cellular metabolism and  
72 physiology, it is not surprising that mutations in mitochondrial carriers have been associated  
73 with a large number of pathologies. Due to recent advances in sequencing technologies, this  
74 number is likely to rise rapidly, as new links to disease are discovered frequently, including  
75 for mitochondrial carriers that have no assigned function yet. Although originally thought to  
76 be relatively rare, it is now clear that pathologies involving mitochondrial carriers may be  
77 among the most prevalent of all mitochondrial diseases. For example, citrin deficiency,  
78 which is caused by disease variants of the mitochondrial aspartate/glutamate carrier  
79 (SLC25A13), has a very high frequency in Far Eastern populations (146). Current estimates,  
80 based on pathogenic allele frequencies, are 1:17,000 in Japan and China, 1:9,000 in Taiwan,  
81 and 1:50,000 in Korea, but the disease has now also been discovered in other populations,  
82 making it panethnic (38, 122). With few exceptions most pathologies are inherited in an  
83 autosomal recessive manner. The phenotypic manifestation of these pathologies is highly  
84 variable, starting at different ages, affecting various organs in different ways, and is  
85 dependent on the type of mutation, i.e. deletion, missense, nonsense, inversion, or splice-  
86 site mutation. The pathologies can be broadly divided into developmental, metabolic and  
87 neuromuscular diseases. Understanding the molecular basis for these diseases is vital for  
88 diagnosis and prognosis of the disease, and for development of effective treatments and  
89 therapies.

90

91         In this review, we provide a comprehensive overview of the role of mitochondrial  
92 carriers in physiology and pathology. We describe all pathogenic missense mutations that  
93 have been identified to date in the context of new insights into the structural mechanism of  
94 these transport proteins. This analysis can be used to predict with better accuracy which  
95 mutations are likely to be pathological, resulting in a dysfunctional mitochondrial carrier.

96 The data presented in this review may also help to identify new pathological variants and  
97 associated mitochondrial diseases.

98

## 99 **The role of mitochondrial carriers in physiology and pathology**

100 With its 53 members, the mitochondrial carrier family SLC25 is the largest solute transporter  
101 family in humans. Here, we first briefly review the function of the known human  
102 mitochondrial carriers in cellular physiology and pathology, but for more detailed  
103 information the reader is referred here (124).

104

### 105 **Nucleotide transport**

106 Mitochondria require nucleotides for a host of important functions, such as the synthesis of  
107 ATP, mitochondrial RNA and DNA synthesis, enzymatic reactions, and regulation. The best-  
108 known member of the SLC25 family is the mitochondrial ADP/ATP carrier, also called  
109 adenine nucleotide translocase or translocator (ANT). The carrier imports ADP into the  
110 mitochondrial matrix, where it is converted to ATP by ATP synthase, and exports the newly  
111 synthesized ATP to the cytosol, where it fuels the metabolic energy-requiring processes that  
112 are vital for cell survival (7, 83, 90, 144). There are four different paralogs in humans, AAC1,  
113 AAC2, AAC3 and AAC4 (SLC25A4, SLC25A5, SLC25A6 and SLC25A31, respectively), which are  
114 expressed in a tissue-dependent manner (FIGURE 1A) (31, 40, 88, 115). The mitochondrial  
115 ADP/ATP carriers carry out equimolar exchange of ADP and ATP, and thus do not alter the  
116 total adenine nucleotide pool in the mitochondrial matrix. The mitochondrial ADP/ATP  
117 carrier has been extensively characterized structurally (FIGURE 2A) (128, 141-144). In the  
118 absence of adenine nucleotides and in the presence of fatty acids, the mitochondrial  
119 ADP/ATP carrier may function as an uncoupling protein, transporting protons (13, 20), but a  
120 molecular mechanism is lacking.

121 The human mitochondrial ADP/ATP carrier AAC1 (SLC25A4) has three associated  
122 pathologies, which are quite different in nature: (i) late onset dominant progressive external  
123 ophthalmoplegia with mitochondrial DNA deletions (OMIM 609283) (77), (ii) recessive  
124 mitochondrial DNA depletion syndrome (OMIM 615418) (53, 125), and (iii) early-onset  
125 dominant *de novo* mutations leading to mitochondrial disease, varying from lethal to mild  
126 severity (OMIM 103220) (81, 158). The complexity of the genetics underlying these three  
127 diseases has not been fully explained. As will be shown below, the carrier has all the features



128 required for its transporter function, so the dominant inheritance cannot be explained by  
129 dimerization, as was thought previously (91). This notion is supported further by the fact  
130 that the early-onset dominant disease mutations involve key functional residues on the  
131 inside of the carrier, which cannot be involved in dimerization (158). Every day the ADP/ATP  
132 carriers transport approximately our own body weight in ADP and ATP across the inner  
133 membrane of mitochondria, meaning that the dominant inheritance could well be explained  
134 by haplo-insufficiency. In agreement, the early-onset *de novo* dominant mutations affect  
135 highly conserved residues that are central to the transport mechanism (p.Lys33Gln,  
136 p.Arg80His and p.Arg235Gly), whereas late-onset domain mutations affect non-conserved  
137 residues on the periphery of the protein without an obvious role in the mechanism (e.g.  
138 p.Ala90Asp, p.Asp104Gly, Leu98Pro, and Ala114Pro). Not fitting this genetic explanation are  
139 the recessive mutations, which lead to mitochondrial DNA deletions and mitochondrial  
140 disease only in homozygotes, whereas the heterozygotes are unaffected (53), but they may  
141 give rise to biogenesis rather than functional issues (e.g. p.Ala123Asp, p.Arg263Pro).  
142 However, it would be impossible for humans to live without functional ADP/ATP carriers, as  
143 cells would be reliant on glycolysis and fermentation alone, providing low yields of ATP. The  
144 oxidative phosphorylation of sugars, fats and amino acids in mitochondria is critically  
145 dependent on ADP/ATP carriers. This notion is supported by the fact that the powerful  
146 inhibitors carboxyatractyloside and bongkreikic acid kill humans, showing that human life  
147 cannot sustain itself without mitochondrial ADP/ATP transport. There are three other  
148 paralogs of the mitochondrial ADP/ATP carrier, AAC2, AAC3, and AAC4, which are expressed  
149 at different levels and/or may be upregulated to compensate for the missing transport  
150 activity in homozygous recessive patients. In addition, there are the four paralogs of the  
151 ATP-Mg/Pi carrier and some vitamin transporters, such as the CoA transporter (SLC25A42)  
152 (51) and thiamine pyrophosphate carrier (SLC25A19) (39), which can also transport adenine  
153 nucleotides in addition to their key substrates. The complexity of adenine nucleotide  
154 transport might explain viability in the homozygous recessive cases and the variation in  
155 severity and onset of the pathogenicity in the heterozygous dominant cases (81, 158). The  
156 mitochondrial ADP/ATP carrier can also transport the deoxy forms of ADP and ATP, which  
157 are required for mitochondrial DNA replication, which could explain the role of disease  
158 variants in mitochondrial DNA deletions and maintenance, aside from the production of ATP.  
159 Finally, very little is known about the effect of these mutations on the biogenesis of the

160 disease variants. Therefore, other genetic mechanisms, such as gain of function through  
161 aggregation, are also pursued as an explanation (100, 101). However, it is clear that this  
162 important issue is unresolved, requiring a more complete picture of adenine nucleotide  
163 transport in mitochondria.

164 The net import and export of adenine nucleotides is carried out by mitochondrial  
165 ATP-Mg/Pi carriers, which exchange phosphate for adenine nucleotides, coupled to  
166 magnesium or protons, in an electroneutral way (8, 36, 45). This transport activity allows the  
167 mitochondrion to respond to changes in energetic demand and to replenish adenine  
168 nucleotide pools after mitochondrial division and macromolecular synthesis (8, 26, 45).  
169 There are three human paralogs APC1 (SLC25A24), APC2 (SLC25A23), APC3 (SLC25A25),  
170 which are calcium-regulated (5, 45), and a fourth isoform APC4 (SLC25A41), which is not  
171 (160) (FIGURE 1B). APC1-3 have three domains; (i) an N-terminal calcium-regulatory domain  
172 with four calcium-binding EF-hands, (ii) an amphipathic helix and (iii) a C-terminal carrier  
173 domain (59) (FIGURE 2B). In the current model of calcium regulation, the amphipathic helix  
174 is bound to the regulatory domain in the presence of calcium, allowing transport by the  
175 carrier domain to occur (59, 169). In the absence of calcium, the amphipathic helix is  
176 released from the regulatory domain and binds to the carrier domain, leading to inhibition of  
177 transport (58, 60). APC4 lacks both the N-terminal calcium-regulatory domain and the  
178 amphipathic helix (160), which accounts for the absence of calcium regulation.

179 Dysfunction of the mitochondrial Mg-ATP/phosphate carrier APC1 (SLC25A24) leads  
180 to Fontaine Progeroid Syndrome, also described as Gorlin–Chaudhry–Moss or Fontaine–  
181 Farriaux syndrome (43, 138, 145, 168) (OMIM 612289). The mutations are spontaneous  
182 rather than inherited, and lead to a developmental disease, which is characterized by  
183 prenatal and postnatal growth retardation, failure to thrive, a lack of subcutaneous adipose  
184 tissue, premature closure of certain skull bones (coronal craniosynostosis) and short distal  
185 phalanges of the fingers and toes. Other clinical features include abnormal hair patterns,  
186 skin agenesis, umbilical hernia and progeroid facial appearance. APC1 variants are expressed  
187 in mitochondria, and they affect both the mitochondrial morphology and cell viability. There  
188 is also a decrease in mitochondrial ATP synthesis in fibroblasts, but only under stress  
189 conditions (168). The disease variants have not been characterized with respect to folding  
190 and transport function. Interestingly, the paralogue APC3 (SLC25A25) has been implicated in  
191 left-right determination during development and is regulated by TRPP2 ion channels (64),

192 showing that the Mg-ATP/phosphate carrier are also playing an important role in  
193 development.

194         There are two pyrimidine nucleotide carriers in humans (PNC1, SLC25A33 and PNC2,  
195 SLC25A36), which are required for mitochondrial DNA and RNA synthesis and breakdown  
196 (37, 52) (FIGURE 1C). SLC25A33 transports uracil, thymine, and cytosine (deoxy)nucleoside  
197 di- and tri-phosphates by an antiport mechanism, whereas SLC25A36 translocates both  
198 cytosine and uracil (deoxy)nucleoside mono-, di and tri-phosphates using a uniport or  
199 antiport mechanism (37, 52). Both carriers also transport guanine nucleotides, but not  
200 adenine (deoxy)nucleotides. It has also been claimed that the pyrimidine carriers are  
201 involved in the uptake of zinc ions (85), even though several dedicated zinc transporters are  
202 likely to exist in mitochondria. In yeast, a separate mitochondrial GTP/GDP carrier has been  
203 identified (162), but an equivalent transporter has not been identified in humans. The most  
204 closely related carriers by sequence comparison are SLC25A51 and SLC25A52 (137), but no  
205 experimental data are available to support this notion. So far, no disease variants of PNC1  
206 and 2 have been identified.

207

#### 208 **Amino acid transport**

209 Amino acids need to be transported into mitochondria for mitochondrial protein synthesis  
210 and for amino acid interconversion and degradation, which can generate metabolic energy.  
211 Several mitochondrial amino acid transporters have been identified, but some are still  
212 missing, importantly those for tryptophan, tyrosine, phenylalanine, methionine, glutamine,  
213 asparagine and cysteine (FIGURE 1D).

214         The mitochondrial aspartate/glutamate carriers import glutamate and a proton, and  
215 they export aspartate from the mitochondrial matrix (9, 16, 18). AGC1 (SLC25A12, aralar)  
216 and AGC2 (SLC25A13, citrin) are expressed in excitable and non-excitable tissues,  
217 respectively, and play important roles in the malate-aspartate shuttle (FIGURE 1E),  
218 gluconeogenesis, purine and pyrimidine synthesis, the urea cycle (AGC2) (FIGURE 1F) and  
219 myelin synthesis (AGC1) (126). They have an unusual three-domain structure, consisting of  
220 (i) a N-terminal calcium-regulatory domain, (ii) a carrier domain, and (iii) a C-terminal  
221 amphipathic helix (157) (FIGURE 2C). The N-terminal domain has eight EF-hand domains, but  
222 only EF-hand 2 is capable of binding calcium, whereas EF-hands 4-8 are involved in  
223 dimerization, generating a structural homo-dimer (FIGURE 2C). In the calcium-bound state,

224 the amphipathic helix is bound to the regulatory domain, whereas in the absence of calcium  
225 the amphipathic helix is released (157), but the mechanism of regulation is not fully  
226 resolved.

227 Mutations of the gene coding for the liver paralog AGC2 (SLC25A13) causes neonatal  
228 and/or adult-onset type-II citrullinemia (OMIM 603859), an autosomal recessive disease  
229 characterized by hyperammonemia and citrullinemia, because of a dysfunctional urea cycle,  
230 as well as neuropsychiatric symptoms and fatty liver disease in later life (86, 122). Mutations  
231 of the gene coding for the brain-specific paralog AGC1 (SLC25A12) lead to early infantile  
232 epileptic encephalopathy due to hypomyelination (OMIM 603667). This is caused by the lack  
233 of mitochondrial aspartate export, which is required for the synthesis of N-acetyl-aspartate,  
234 a precursor for myelin synthesis (167).

235 Two related proteins, the mitochondrial glutamate carriers GC1 (SLC25A22) and GC2  
236 (SLC25A18), are involved in the import of glutamate together with a proton, but do not  
237 export aspartate (FIGURE 1D) (50). The glutamate carriers do not have the calcium-  
238 regulatory elements found in aspartate/glutamate carriers. Mutations in SLC25A22 (OMIM  
239 609302) cause neonatal epileptic encephalopathy with suppression bursts (97, 110), or  
240 migrating partial seizures in infancy with poor developmental prognosis (129). The most  
241 likely reason for the disease phenotype is the role of mitochondrial glutamate transport in  
242 sustaining glutamate homeostasis in astrocytes (55).

243 The glycine carrier GLYC (SLC25A38) is involved in the import of glycine into  
244 mitochondria, where it reacts enzymatically with succinyl-CoA to form aminolevulinic acid  
245 (FIGURE 1G) (102). The gene was flagged up because a disease variant leads to autosomal  
246 recessive sideroblastic anemia (OMIM 610819), caused by the inability of blood cells to  
247 synthesize heme due to defective glycine transport (48). Aminolevulinic acid is transported  
248 by an unknown transporter into the cytosol, where it is used as a precursor for porphyrin  
249 synthesis. The resulting coproporphyrinogen III is then transported into mitochondria by an  
250 unknown transporter for incorporation of iron and insertion into heme-containing proteins.

251 The ornithine carriers ORC1 and ORC2 (SLC25A15 and SLC25A2) catalyze the  
252 exchange of ornithine and citrulline, which links the fixation of ammonia in mitochondria to  
253 the urea cycle (FIGURE1H) (47). The substrate specificity and binding of these two paralogs  
254 have been studied in detail (111). Dysfunction of ORC1 (SLC25A15) leads to HHH syndrome  
255 (OMIM 603861), characterized by hyperornithinemia, hyperammonemia and

256 homocitrullinuria, due to an impaired urea cycle, which is required for the deamination of  
257 amino acids (22, 65). *ORC2* (*SLC25A2*) (OMIM 608157) may be responsible for the milder  
258 phenotype in HHH patients, secondary to a gene redundancy effect. The basic amino acid  
259 carrier *BAC* (*SLC25A29*) is closely related to *ORC1* and 2, but transports arginine, lysine,  
260 homoarginine, methylarginine and, to a much lesser extent, ornithine and histidine (131)  
261 and has thus far no pathology associated with it.

262 Recently, the mitochondrial carrier for branched-chain amino acids (*SLC25A44*) was  
263 identified (FIGURE 1D) (171). The branched-chain amino acids valine, leucine and isoleucine  
264 can be degraded to provide metabolic energy and are required for the synthesis of proteins  
265 in mitochondria. The carrier was discovered in brown adipose tissue upon cold exposure,  
266 where branched-chain amino acids can be used as a fuel for thermogenesis.

267

#### 268 **Vitamin transport**

269 Many vitamins need to be transported into mitochondria, where they serve as co-factors or  
270 as donors of key functional groups in the enzymatic reactions of the mitochondrial matrix  
271 (FIGURE1I).

272 The mitochondrial *S*-adenosylmethionine carrier *SAMC* (*SLC25A26*) imports *S*-  
273 adenosylmethionine into mitochondria, which is required for methylation reactions of DNA,  
274 RNA and protein in the mitochondrial matrix, and exports the product *S*-  
275 adenosylhomocysteine (3). A missense mutation in the gene coding for this protein causes  
276 intra-mitochondrial methylation deficiency (OMIM 611037) in agreement with this function,  
277 leading to oxidative phosphorylation deficiency (82).

278 The human thiamine pyrophosphate transporter *TPC* (*SLC25A19*) was initially  
279 identified as a deoxynucleotide transporter (39), but its main function is the transport of  
280 thiamine pyrophosphate, which is an important co-factor in dehydrogenase reactions (99).  
281 Defective transport of thiamine pyrophosphate is the cause of Amish microcephaly, which is  
282 characterized by profound congenital microcephaly, delayed psychomotor development,  
283 lactic and alpha-ketoglutaric aciduria (OMIM 606521) (78). A second mutation was reported  
284 in siblings of non-Amish background (OMIM 613710), expanding the phenotypes associated  
285 with the *SLC25A19* gene. These patients showed recurrent episodes of flaccid paralysis and  
286 encephalopathy associated with bilateral striatal necrosis and chronic progressive  
287 polyneuropathy caused by a missense mutation in *SLC25A19* (155).

288 Mitochondria require folate for one-carbon metabolism and flavins for electron  
289 transfer steps in the respiratory chain. The transport of folate and flavin have both been  
290 assigned to a single mitochondrial carrier (SLC25A32) (154, 159). The substrate binding site  
291 has typical features of an adenine binding pocket, agreeing with the flavin assignment (94,  
292 136, 137). When mutated, the disease variant of this carrier causes exercise intolerance  
293 (OMIM 610815) and riboflavin supplementation proved to be beneficial to the patients,  
294 indicating that the most likely substrate of this carrier is flavin rather than folate (149).

295 Many reactions in the mitochondrial matrix, such as dehydrogenase activities,  
296 require coenzyme A (CoA) as co-factor. Coenzyme A is synthesized outside of mitochondria  
297 and must be transported into the mitochondrial matrix. The CoA transporter (SLC25A42) was  
298 initially identified based on database searches and showed expression in all tissues with the  
299 highest levels detected in adipose tissue, and high levels detected in hypothalamus and all  
300 brain coronal sections (57). The disease variant of the CoA transporter (OMIM 610823)  
301 causes mitochondrial myopathy with muscle weakness and lactic acidosis, while other  
302 tissues and cognitive functions are not impaired (150). Another report described variable  
303 clinical manifestations, including lactic acidosis, developmental regression and epilepsy (4).

304 Before SLC25A42 was identified as the CoA transporter, this transport activity was  
305 putatively assigned to protein encoded by the *SLC25A16* gene (133). Both SLC25A16 and  
306 SLC25A42 are phylogenetically related to the yeast protein Leu5p and are capable of  
307 complementing the yeast knockout strain (51). The function and kinetic parameters of  
308 SLC25A42 were determined in transport assays with substrate specificities restricted to CoA,  
309 dephospho-CoA, ADP, and adenine-3',5'-diphosphate (51). The human protein encoded by  
310 the *SLC25A16* gene has been identified through a possible association with a thyroid disease  
311 called Grave's disease, but it has not been demonstrated that it can transport CoA (173). To  
312 date only a single homozygous mutation has been reported in the *SLC25A16* gene (OMIM  
313 139080) causing a nail disorder of the hand with different severity levels of onychodystrophy  
314 (79), but a direct correlation to function has not been confirmed either.

315

### 316 **Inorganic ion transport**

317 Inorganic ions also need to be transported into the mitochondrial matrix, where they  
318 function as co-factors, as substrates for enzymatic reactions and as regulators. There are

319 likely to be transporters of other families as well as channels involved in inorganic ion  
320 transport, but they are beyond the scope of this review.

321         The mitoferrins SLC25A37 (MFRN1) and SLC25A28 (MFRN2) have been proposed to  
322 transport iron ions into mitochondria for incorporation into heme and iron-sulfur cluster  
323 synthesis, as well as other functions (FIGURE 1J) (113, 151). MFRN1 is highly expressed in  
324 differentiating erythroid cells and in other tissues at low levels, while MFRN2 is expressed  
325 ubiquitously in non-erythroid tissues (29, 151). Abnormal MFRN1 expression might  
326 contribute to erythropoietic protoporphyria phenotype in agreement with this notion (165).

327         The mitochondrial phosphate carrier PIC (SLC25A3) imports inorganic phosphate for  
328 the synthesis of ATP (140) together with a proton (FIGURE 1K) (95). There are two  
329 alternative splicing variants showing different kinetic parameters and different expression  
330 profiles: while isoform A is highly expressed in heart, skeletal muscle, diaphragm (49), and  
331 pancreas (67), isoform B is expressed in all tested tissues, i.e., lung, kidney, brain, thymus,  
332 liver, heart, skeletal muscle, and diaphragm (49), albeit at lower levels compared to isoform  
333 A (67). The phosphate carrier is fundamental in maintaining the inorganic phosphate pool in  
334 the mitochondrial matrix, but there are also other carriers capable of transporting  
335 phosphate, such as the dicarboxylate carrier DIC (SLC25A10) and mitochondrial ATP-Mg/Pi  
336 carriers APC1 (SLC25A24), APC2 (SLC25A23), APC3 (SLC25A25), and APC4 (SLC25A41) (5, 45,  
337 160). Phosphate carrier deficiency leads to lactic acidosis, hypertrophic cardiomyopathy, and  
338 muscular hypotonia and early mortality (OMIM 600370) in agreement with the notion that  
339 its transport activity is the main pathway for phosphate import for ATP synthesis (15, 105,  
340 106).

341

#### 342 **Fatty acid transport**

343         The carnitine/acylcarnitine carrier CAC (SLC25A20) is a key component of the carnitine cycle  
344 and imports acyl-carnitine into mitochondria for fatty acid  $\beta$ -oxidation and exports carnitine  
345 (FIGURE1L) (66, 70). Mutations cause carnitine/acylcarnitine carrier deficiency, an autosomal  
346 recessive disorder characterized by severe, neonatal onset with cardiomyopathy or a milder  
347 phenotype with hypoglycemia, but no cardiomyopathy (OMIM 613698) (66). The inability to  
348 transport fatty acid chains into mitochondria makes the patients dependent on  
349 carbohydrates and amino acids for energy metabolism.

350

### 351 **Uncoupling protein**

352 The uncoupling protein UCP1 (SLC25A7) is predominantly found in brown adipose tissue of  
353 neonatal mammals (6, 118, 120), but is also found in the supraclavicular and the neck  
354 regions in adults in later life (FIGURE 1M) (116). UCP1 dissipates the proton motive force,  
355 short-circuiting the mitochondrion, which leads to the production of heat. The generation of  
356 heat from the oxidation of brown adipose fat protects the newly born against cold stress of  
357 vital organs. UCP1 is activated by fatty acids and inhibited by purine nucleotides (134), but  
358 the mechanism is still debated (23, 33, 44, 72, 84, 119). UCP1 is monomeric and binds three  
359 cardiolipin and a single purine nucleotide (96). Based on sequence analysis, UCP1 has  
360 retained all of the key features of mitochondrial carriers, indicating that it operates by a  
361 conventional carrier-like mechanism (33, 96). The transport of protons induced by fatty acids  
362 is relatively slow (44), which would fit a transporter rather than a channel mechanism, but a  
363 molecular mechanism has not been resolved. Although there are other closely related  
364 proteins (see below), UCP1 is most likely the only one involved in thermogenesis. There are  
365 no known disease states associated with mutations in the gene coding for UCP1.

366

### 367 **Dicarboxylate transport**

368 Dicarboxylates (FIGURE 1N) need to be continuously exchanged across the mitochondrial  
369 inner membrane for many different pathways, such as the tricarboxylic acid cycle,  
370 malate/aspartate shuttle, gluconeogenesis, and amino acid metabolism.

371 The mitochondrial dicarboxylate carrier DIC (SLC25A10) is involved in the transport of  
372 malonate, malate, succinate, sulphate, thiosulphate, and phosphate by electroneutral  
373 exchange (46, 73). The carrier is involved in gluconeogenesis and ureogenesis, the  
374 metabolism of sulfur compounds, as well as in *de novo* fatty acid synthesis (109). The  
375 mitochondrial oxoglutarate carrier OGC (SLC25A11) exchanges cytosolic malate for 2-  
376 oxoglutarate from the mitochondrial matrix and plays an important role in the malate-  
377 aspartate shuttle, the oxoglutarate-isocitrate shuttle, and gluconeogenesis (69). Mutations  
378 in the gene might be correlated to metastatic paragangliomas (21).

379 The oxodicarboxylate carrier ODC (SLC25A21) import 2-oxoadipate and exports 2-  
380 oxoglutarate, playing a central role in the catabolism of lysine, hydroxylysine and tryptophan  
381 (FIGURE 1O) (48). Oxodicarboxylate carrier deficiency (OMIM 607571) is associated with



382 mitochondrial DNA depletion and spinal muscular atrophy-like disease, most likely caused by  
383 the accumulation of toxic amino acid breakdown products (17).

384         There are several closely related sequences to UCP1, such as UCP2 (SLC25A8), UCP3  
385 (SLC25A9), UCP4 (SLC25A27), UCP5 (SLC25A14), and UCP6 (SLC2530), but they are likely to  
386 be transporters of carboxylic acids (54, 163), which is in agreement with their close  
387 phylogenetic relationship to dicarboxylate transporters (123) and with the properties of  
388 their substrate binding sites (137). Many unresolved questions remain with respect to their  
389 molecular properties and their role in thermogenesis and metabolism. There are also other  
390 potential dicarboxylate carriers, such as SLC25A34 and SLC25A35, but their role in  
391 metabolism has not been clarified.

392

### 393 **Tricarboxylate transport**

394 The tricarboxylate or citrate carrier (SLC25A1) catalyzes the electroneutral exchange of  
395 tricarboxylates (citrate, isocitrate) for another tricarboxylate, a dicarboxylate or  
396 phosphoenolpyruvate (68, 76, 103). An important physiological function is the export of  
397 citrate from the mitochondria to the cytosol for the production of acetyl CoA, which is a  
398 starting point for lipid, dolichol, ubiquinone and sterol synthesis (references in (103)), and  
399 acetylation reactions (112) (FIGURE 1P). Citrate carrier deficiency (OMIM 190315), which is  
400 hallmarked by combined D-2- and L-2-hydroxyglutaric aciduria, leads to neonatal-onset  
401 epileptic encephalopathy with severe muscular weakness, respiratory distress, and lack of  
402 psychomotor development resulting in early death (30, 42, 114, 121, 132, 152), which is  
403 most likely due to the severe biosynthetic deficiencies (103). Many of the missense  
404 mutations have been characterized with respect to the function of SLC25A1 (27, 42, 103,  
405 130).

406

### 407 **Apoptosis**

408 SLC25A50 (MTCH2) is a partially characterized mitochondrial carrier, which acts as a  
409 receptor-like protein for the truncated BH3-interacting domain death agonist protein in the  
410 outer membrane of mitochondria, as part of the apoptosis pathway (FIGURE 1Q) (172).  
411 MTCH2 is likely to have a similar topology as other mitochondrial carriers (135), but  
412 unusually it is found in the mitochondrial outer membrane. A transported substrate has not

413 yet been identified, if this protein has a transporter function at all, but MTCH2 was  
414 subsequently found to be required and sufficient for lipid homeostasis shifts (139).

415

#### 416 **Mitochondrial dynamics**

417 The partially characterized mitochondrial carrier SLC25A46 is most likely involved in  
418 mitochondrial dynamics (FIGURE 1R). Overexpression leads to mitochondrial fragmentation,  
419 whereas knockdown results in hyperfilamentous mitochondria and mitochondrial  
420 hyperfusion, likely resulting from decreased fission. Loss of SLC25A46 was not associated  
421 with changes in total ATP concentration, mitochondrial DNA content, or membrane  
422 potential (2). SLC25A46 could interact with proteins associated with mitochondrial  
423 dynamics, such as OPA1 and MFN2, and with components of the mitochondrial contact site  
424 and mitochondrial cristae organizing system complex, which plays a role in cristae  
425 maintenance (71). SLC25A46 might also interact with components of an endoplasmic  
426 reticulum membrane protein complex involved in lipid transfer to mitochondria, which are  
427 also required for cristae growth and maintenance. SLC25A46 is found in the outer  
428 membrane of mitochondria (71), which is atypical for mitochondrial carriers except for  
429 MTCH2 (see above). It is possible that the carrier has evolved away from the canonical  
430 transporter function, as, so far, no substrates have been identified. Disease variants of  
431 SLC25A46 (OMIM 610826) lead to hereditary motor and sensory neuropathy type VIB (2)  
432 and in severe cases to death in infancy (1, 164).

433

#### 434 **Uncharacterized mitochondrial carriers**

435 The functions of a large number of mitochondrial carriers have not yet been assigned,  
436 limiting our understanding of their role in human physiology and pathology. Among them  
437 are SLC25A34, SLC25A35, SLC25A39, SLC25A40, SLC25A43, SLC25A45, SLC25A47, SLC25A48,  
438 SLC25A49 (MTCH1), SLC25A51 (MCART1), SLC25A52 (MCART2) and SLC25A53 (MCART6),  
439 which is roughly a quarter of the total. No substrates have been identified for SLC25A46 and  
440 SLC25A50 (MTCH2) (see above), although they have a role in mitochondrial dynamics and  
441 apoptosis, respectively. There is still a lot of debate on the role of UCP2 (SLC25A8), UCP3  
442 (SLC25A9), UCP4 (SLC25A27), UCP5 (SLC25A14), and UCP6 (SLC2530) in human physiology. In  
443 some other cases, the function of particular carriers has been disputed, for example

444 SLC25A32, which has been described as a folate or flavin transporter. Counting these, the  
445 number of carriers that are not yet fully characterized is closer to a third of the total.

446

### 447 **The molecular basis of pathogenic missense mutations**

448 Missense mutations in 16 different carriers lead to human disease, but it is likely that this  
449 number will increase substantially as more links are discovered through genome and exome  
450 sequencing. These mutations can impair the structure and mechanism of the carrier, but can  
451 also cause issues with biogenesis, i.e. the expression, targeting, insertion and folding of the  
452 disease variant. The impact of the vast majority of these missense mutations on the  
453 structure, function and biogenesis of the carrier has not been studied experimentally. To  
454 discriminate between these different scenarios, it is important to understand the transport  
455 mechanism in detail. Recently, good progress has been made facilitating this assessment,  
456 although many details still need to be worked out. To explain the molecular impact of the  
457 pathogenic mutations on the function of mitochondrial carriers, it is important to explain  
458 their basic structure and transport mechanism first.

459

### 460 **Structures of mitochondrial carriers**

461 Mitochondrial carriers consist of three homologous repeats of about one hundred amino  
462 acid residues each (FIGURE 3A) (147). The three repeats fold up into a three-fold pseudo-  
463 symmetrical fold, noted first in the projection structure of the yeast ADP/ATP carrier Aac3p  
464 (92). This study also demonstrated that the carrier had a monomeric structure and a  
465 translocation path for substrates through the center of the protein (92). The first atomic  
466 structure of the bovine ADP/ATP carrier provided the first evidence for the basic structural  
467 topology of all mitochondrial carriers (128). Each repeat or domain has an odd-numbered  
468 helix (H1, H3, H5), a matrix loop of variable length, a matrix helix (h12, h34, h56), a linker  
469 helix (l12, l34, l56), and an even-numbered helix (H2, H4, H6) (128) (FIGURE 3A and B). The  
470 domains are linked by cytoplasmic loops, which are located in the intermembrane space,  
471 together with the N- and C-termini. The structure was locked by the specific inhibitor  
472 carboxyatractyloside in the cytoplasmic state in which the central cavity is open to the  
473 intermembrane space and via channels to the cytoplasm, for binding of ADP (FIGURE 4)  
474 (128). Although there are some structural differences, the same basic structural fold was  
475 observed for the yeast ADP/ATP carrier Aac2p and Aac3p, even though they share only ~50%

476 identity with the bovine carrier (141). More recently, the atomic structure of the  
477 mitochondrial ADP/ATP carrier inhibited by bongkreikic acid was solved, locked in the matrix  
478 state in which the central cavity is open to the mitochondrial matrix, for binding of ATP  
479 (FIGURE 4) (142, 144). The central cavity in both states is positively charged, primed for  
480 binding of the negatively charged adenine nucleotides (128, 142, 144). The residues of the  
481 substrate binding site have been identified by computational methods, using chemical and  
482 distance constraints in comparative models (94, 136), deviation of symmetry (95, 137), or  
483 molecular dynamics simulations (35, 107, 166). The three main contact points involved in  
484 substrate binding are located on the even-numbered helices (FIGURE 4) (94, 136). The  
485 substrate binding site is located at the bottom of a water-filled cavity in both states, which  
486 corresponds to the middle of the membrane (94, 136). There are two gates on either side of  
487 the carrier that regulate access to the central binding site. In the cytoplasmic state, the  
488 matrix gate is closed and the cytoplasmic gate is open, whereas in the matrix state, the  
489 cytoplasmic gate is closed and the matrix gate is open (FIGURE 4) (142-144). Each closed  
490 gate is about 15-Å thick, an important insulation layer to prevent the leak of protons and  
491 other ions in the presence of a 180-mV membrane potential. These gates contain salt bridge  
492 networks of positively and negatively charged amino acid residues and other features, which  
493 will be discussed later.

494

#### 495 **Transport mechanism of mitochondrial carriers**

496 Comparison of the two inhibited states has revealed the basic structural mechanism of  
497 transport and has completed our understanding of the importance of key conserved  
498 sequence features of the SLC25 family for the transport mechanism (FIGURE 5) (142-144).  
499 The two inhibitors occupy the proposed substrate binding site of the carrier, preventing  
500 substrate binding, but also induce slight conformational changes, which lock the carrier  
501 permanently in an abortive state (142). These distortions can be corrected for structurally to  
502 achieve a closer approximation of the unliganded states, which are used in this review. A  
503 morph between the unliganded states passes through an occluded state, where access to  
504 the substrate binding site is blocked from both sides of the membrane, which is a  
505 requirement for an alternating access transport mechanism (142).

506 Further analysis shows that most of the domain structure is conserved between the  
507 two states, i.e. the odd-numbered helix, the matrix helix, the linker helix and a third of the

508 even-numbered helix (142-144). These parts of the domain are called the core elements, and  
509 are shown in primary colors, blue, yellow and red for the first, second and third domain,  
510 respectively (FIGURE 5). In contrast, a significant change occurs in the position of the C-  
511 terminal regions of the even-numbered helices in the state interconversion (143, 144). These  
512 parts of the structure are called the gate elements, and they are shown in gray (FIGURE 5).  
513 The hinge points of these movements turned out to be the contact points of the proposed  
514 substrate binding site (142-144), identified previously (94, 136). Opening or closing of the  
515 matrix side of the carrier involves the rotation of the three core elements as rigid-bodies,  
516 whereas opening or closing of the cytoplasmic side requires the rotation of three gate  
517 elements. In this way, access to the central substrate binding site from one or the other side  
518 of the membrane is alternated (FIGURE 5). The substrate binding site is the fulcrum of these  
519 movements (142-144). Thus, state interconversion requires the coordinated movement of  
520 six elements simultaneously, making the mitochondrial carriers one of the most dynamic of  
521 all transport proteins. These movements are facilitated by the transmembrane helices being  
522 held together only by relatively weak van der Waals interactions. Next, the sequence  
523 features of mitochondrial carriers are examined to determine why they are crucial to the  
524 structure and transport mechanism, as they are often altered in pathogenic variants.

525

#### 526 **Key sequence features affected by pathogenic mutations**

527 The easiest way to present the sequence features of mitochondrial carriers is to use their  
528 three-fold pseudo-symmetry (FIGURE 3). The three repeats are homologous to each other,  
529 meaning that residues that are in the same position in each repeat are symmetry-related  
530 and thus mostly identical or similar in physiochemical properties (137). These residues can  
531 be grouped together in a triplet of symmetry-related residues, which facilitates their  
532 comparison (FIGURE 3A). Here, we have used the residue numbering of the human ADP/ATP  
533 carrier 1 (AAC1, SLC25A4), also known as ANT1, to relate the triplet to the original sequence.  
534 For example, the highlighted triplet (cyan sphere) in FIGURE 3A contains residue 8 in repeat  
535 1, residue 113 in repeat 2, and residue 210 in repeat 3 (FIGURE 3). For convenience, the  
536 entire triplet is named by the residue number in the first repeat in SLC25A4, meaning that  
537 the example above would be called triplet 8. Given the high sequence identity within the  
538 SLC25 family, the same triplets in carriers with different functions can be compared to look

539 for ones that are conserved throughout the family, and are therefore universally important  
540 for the structure and mechanism of mitochondrial carriers (137).

541 FIGURE 6 shows the triplets of all conserved helical features for the 16 mitochondrial  
542 carriers that have been linked to human disease, as well as the reported pathogenic  
543 mutations. The mutations that have been experimentally verified to have a severe effect on  
544 function are shown in red boxes, whereas those that have milder effects are in yellow ones.  
545 Mutations shown in blue boxes have been flagged up in genetic analysis, but their effect on  
546 function has not been studied experimentally. It is clear that mutations affect a large  
547 number of triplets. Next, starting from the N-terminus, these features will be presented by  
548 highlighting the properties of the triplets in relation to the known structural mechanism of  
549 transport (FIGURE 6). The analysis focusses on the conserved helical parts of the carriers, as  
550 the loops are highly variable in length and sequence, and do not play an important role in  
551 the transport mechanism. The most conserved amino acid residues of the triplets are  
552 indicated by the one-letter amino acid code, whereas the most common chemical and  
553 physical properties are also indicated by a one-letter code:  $\pi$  for small residues (Gly, Ala, Ser,  
554 Pro, Cys, Val, Thr),  $\Phi$  for hydrophobic residues (Val, Ile, Leu, Phe, Trp, Tyr, Cys, Ala, and Met),  
555  $\Omega$  for aromatic residues (Trp, Tyr, Phe) and  $\xi$  for hydrophilic residues (Asn, Gln, Glu, Asp, Lys,  
556 Arg, His, Ser, Thr), and X for any residues.

557

#### 558 **Small amino acid residues on the odd-numbered helices**

559 The odd-numbered helices H1, H3 and H5 have a strong kink, giving them an L-shape  
560 (FIGURE 3 and 4) (128). The N-terminal parts are transmembrane and contain a large  
561 number of glycine and other small residues, which are often mutated in disease variants of  
562 the carriers (FIGURE 6). The extended sequence motif is  $\pi G\pi x\pi Gxx\pi xxx\pi$ , where G stands for  
563 glycine and  $\pi$  for small amino acids and x for any amino acid residue (142-144) (FIGURE 7).  
564 These residues can be divided further into two categories: (i) Small residues in the interface  
565 with the preceding helix, i.e. triplets 14, 18, 22, and 26 (pink residues, FIGURE 7), and (ii)  
566 glycine or small residues in the interface with the following helix, i.e. triplets 15 and 19,  
567 which form the GxxxG motif, and triplet 16 (magenta residues, FIGURE 7) (141-144).

568 When the carrier transitions from the cytoplasmic state to the matrix state (FIGURE 4  
569 and 5), the cytoplasmic side of the carrier closes and the transmembrane helices come  
570 together. The reason is that the cytoplasmic side closes because the gate elements rotate

571 inwards, allowing the cytoplasmic network to form (see below). At the same time, the core  
572 elements rotate outwards, and simultaneously the odd helices move inwards on the  
573 cytoplasmic side. The glycine and other small residues of the  $\pi G \pi \kappa \pi G \chi \chi \pi \chi \chi \chi \pi$  motif are in  
574 these crucial interhelical interfaces, allowing movement of the gate elements across the  
575 surface of the odd-numbered helices and the close proximity of the helices in the matrix  
576 state. A large number of pathogenic mutations are observed in these triplets, and functional  
577 and structural analysis shows that these residues are likely to be important for the  
578 mechanism of mitochondrial carriers in general (25, 33, 90). Small residues can also be found  
579 on the even-numbered helices, as will be discussed below.

580 The other triplets found on the transmembrane parts of the odd-numbered helices  
581 preserve their strong amphipathic properties. Triplets 8, 9, 10, 12, 13, 17, 20, 21, 24, and 25  
582 contain mostly generic hydrophobic residues ( $\Phi$  symbols, FIGURE 6), as they point towards  
583 the hydrophobic core of the membrane. Triplets 11, 23, and 27 contain generic hydrophilic  
584 residues ( $\xi$  symbols, FIGURE 6) and point towards the water-filled cavity. Pathogenic  
585 mutations are sporadically observed in these triplets, most likely when they are replaced  
586 with a residue with the opposite properties. For instance, a charged residue for a  
587 hydrophobic one, a large residue for a small one, or a substitution with a proline residue in  
588 the middle of a helix, which could break the helix. These features could be important for  
589 both the function and biogenesis of the carriers.

590

### 591 **Key amino acid residues of the matrix gate**

592 The next important motif on the odd-numbered helices is a highly conserved symmetrical  
593 feature  $Px[DE]xx[RK]xxxQ$  (FIGURE 6). As mentioned above, the odd-numbered helices have  
594 a strong kink of about 50 degrees (FIGURE 5). At this kink is a highly conserved proline  
595 residue (P-kink, triplet 28), the first residue of the motif (128), but it can be replaced by a  
596 serine residue (141). These residues break the hydrogen bond arrangement allowing the  
597 kink to occur and a network of interactions between residues in the domain help to stabilize  
598 it (141) (FIGURE 8). The kinks bring the C-terminal ends of the odd-numbered helices  
599 together in the center of carrier in the cytoplasmic state, where the negatively charged  
600 residues (red residues, triplet 30) and positively charged residues (blue residues, triplet 33)  
601 form an ionic interaction network (117). This interaction network can be seen in the  
602 structure of the cytoplasmic state (128, 141), now called the matrix salt bridge network

603 (137). A glutamine residue (triplet 37) functions as a brace of one of the salt bridge  
604 interactions of the matrix network (glutamine-brace) (green residue, FIGURE 8) (141). Only  
605 one of the three domains of the ADP/ATP carrier has a glutamine brace, but other carriers  
606 have up to three glutamine braces (FIGURE 6). The salt bridge interactions and glutamine  
607 braces together determine the overall interaction energy of the matrix network. Although  
608 not conserved between different carriers, residues in triplet 34 and 38 are in the  
609 translocation path, sealing the carrier to the mitochondrial matrix (FIGURE 6). Together, all  
610 these residues form the matrix gate, which is closed in the cytoplasmic state and open in the  
611 matrix state (FIGURE 5 and 6). In addition, there are triplets with hydrophobic residues  
612 (triplet 29, 32, 36), hydrophilic residues (triplet 34, 38), and residues with varied properties  
613 (triplet 31). This part of the carrier is one of the most important for their function and a large  
614 number of pathogenic variants have been identified in this region (FIGURE 6).

615

#### 616 **Amino acid residues involved in cardiolipin binding**

617 Three cardiolipin molecules are tightly bound to mitochondrial carriers and are important for  
618 their stability and function, as observed by phosphorous NMR experiments (14),  
619 crystallographic analyses (128, 141, 142), lipid analysis (10, 93, 96), disease models (56, 74,  
620 104), thermostability analysis (34), and transport assays (63, 75, 107). The phosphate groups  
621 of cardiolipin are bonded to the N-terminal ends of the matrix and even-numbered helices,  
622 bridging the inter-domain interface (FIGURE 9). Preceding them are highly conserved  
623 symmetrical sequence motifs [YF]XG (triplets 51-53, cardiolipin binding site I) and  
624 [YWF][RK]G (triplets 71-73, cardiolipin binding site II), respectively (FIGURE 6 and 10). The  
625 glycine residues of these motifs (triplets 53 and 73) are in the loop to helix transition, where  
626 they function as helix breakers, but serine, asparagine or threonine can also play this role  
627 (24). This loop to helix transition is crucial for binding of the phosphate groups of cardiolipin  
628 via hydrogen bonds (128) and electrostatic interactions with the helix dipoles (141). Many  
629 pathogenic mutations affect these glycine residues (FIGURE 6). The aromatic residue of  
630 cardiolipin binding site I (triplet 51) is involved in stabilization of the domain on the matrix  
631 side (108), whereas the aromatic residue of cardiolipin binding site II (triplet 71) is involved  
632 in binding the fork of the lipid moiety (128, 141, 142). Although not supported by the  
633 structures, molecular dynamics simulations show that the positive charged residue (triplet  
634 72) might be involved in binding the phosphate moiety via electrostatic interactions (41).



635 Triplet 71-72 have pathogenic mutations, supporting their importance in stability and  
636 function of the carriers.

637

### 638 **Amino acid residues important for the stability of the domain structure**

639 Analysis of all of the polar interactions of the ADP/ATP carrier show that there are no  
640 conserved polar interactions between the transmembrane helices (141), which agrees with a  
641 mechanism where the transmembrane helices move relative to each other in the state  
642 interconversion (FIGURE 5)(142). The only highly conserved interaction is in the domain  
643 structure between a positively charged residue on the odd-numbered helices (E-R link I,  
644 triplet 35) and a negatively charged residue on the matrix helices (E-R link II, triplet 65)  
645 (FIGURE 6 and 11). In the known structures of the ADP/ATP carrier one or two interactions  
646 are evident, supporting the unusual shape of the domain structure (128, 141, 142). One of  
647 the residues of E-R link I in repeat I is a leucine, which cannot be involved in a direct  
648 interaction with the glutamine residue in E-R link II (FIGURE 6). However, a preceding residue  
649 Arg31, which is located one turn of a helix away, is in bonding distance, thus fulfilling the  
650 same role (FIGURE 6). On the basis of sequence analysis, it is likely that all three domains  
651 have this interaction in other carriers, which it has been shown to be important for function  
652 (108).

653 Another residue important for the stability is a tyrosine residue in cardiolipin binding  
654 site I (triplet 51), which forms extra interactions and seals the domain towards the  
655 mitochondrial matrix (FIGURE 10). The E-R link often contains pathogenic mutations, further  
656 supporting its importance.

657 Residues of the matrix helices are strongly amphipathic with polar and charged  
658 residues facing the mitochondrial matrix (triplets 56, 59, 60, 63, 64) and hydrophobic  
659 residues facing the membrane (triplets 54, 55, 58, 61, 62) (FIGURE 6). Small residues are also  
660 required for the stability of the domain structure, as helix breakers, such as glycine residues  
661 (triplet 53, 66, 73), or small residues pointing towards other residues (triplet 57, 69) (FIGURE  
662 11). These areas are affected by pathogenic mutations, likely because the mutations cause  
663 changes to amino acids with opposite biophysical properties.

664

### 665 **Amino acid residues of the substrate binding site**

666 A single substrate binding site can be found in the central cavity, approximately halfway the  
667 membrane. The binding site consists of residues that are directly involved in binding of the  
668 substrate, such as the contact points (FIGURE 4, 5 and 12), but also of residues that allow the  
669 binding of the substrate in the water-filled cavity. This area is a hyper-variable region and  
670 contains a large number of asymmetric residues (137). Most of these residues can be found  
671 on the even-numbered helices at triplets 77, 80 (contact points), 81, 84, and possibly 85.  
672 There are many disease variants that have mutations in this area, and which have been  
673 shown to affect function in functional studies. There are also triplets that often contain  
674 proline residues, such as triplet 76 and 83, which can be found on either side of the contact  
675 points (triplet 80) and may facilitate the curvature or the relative movement of the helices.

676

#### 677 **Small amino acid residues on the even-numbered helices**

678 As explained earlier, the state interconversion requires the presence of small residues in the  
679 interhelical interfaces. Several can be found on the even-numbered helices that facilitate  
680 these movements, such as the aforementioned triplet 76, and a  $\pi$ xxx $\pi$  motif, formed by  
681 triplet 86 and 90 (FIGURE 6 and 13). The even-numbered helices are also highly amphipathic,  
682 containing hydrophobic residues in triplets 74, 75, 78, 79, 82, 87, and 91, facing the  
683 membrane, and hydrophilic residues facing the cavity, such as the substrate binding site  
684 residues, and triplets 88, 94 and 97 (FIGURE 6).

685

#### 686 **Amino acid residues of the cytoplasmic gate**

687 The C-terminal ends of the even-numbered helices contain highly conserved symmetrical  
688 sequence motifs  $\xi$ [FY]xx[YF][DE]xx[RK] (triplets 88-96). Together, they form the cytoplasmic  
689 gate (FIGURE 6). The negative charged residues (triplet 93) and positively charged residues  
690 (triplet 96) form the cytoplasmic salt bridge network, when the carrier is in the matrix state  
691 (80, 142, 144), whereas this network is disrupted in the cytoplasmic state (red and blue  
692 residues, FIGURE 14) (141). The preceding aromatic residue (triplet 92), most often a  
693 tyrosine residue, can form hydrogen bond interactions with the negative charged residue of  
694 the neighboring domain (orange residue, FIGURE 14). This interaction is called the tyrosine  
695 brace, and mitochondrial carriers have one to three of these interactions, modifying the  
696 overall interaction energy of this network. Together with triplet 89, it also doubles up as a  
697 hydrophobic layer when the carrier is in the matrix state. Triplet 88, which is quite variable,

698 is part of the cytoplasmic gate and also forms part of the ceiling of the substrate binding site  
699 (green residues, FIGURE 14). These residues are often mutated in disease variants.

700

### 701 **Concluding remarks**

702 Mitochondrial carriers are highly dynamic transporters, which interconvert between a  
703 cytoplasmic state and a matrix state using six dynamic elements, comprising three core  
704 elements and three gate elements. They are among the smallest transporters in nature, yet  
705 they transport some of the largest molecules, such as adenine nucleotides, S-adenosyl  
706 methionine, flavins and acyl-carnitines. They do so without significant proton leak, because  
707 of a matrix and cytoplasmic gate, both with salt bridge networks and braces, and other  
708 residues that provide an insulation layer. All carriers have a single central substrate binding  
709 site with three contact points, which is alternately accessible from one side of the  
710 membrane or the other, key properties of an alternating access transport mechanism. A  
711 large number of pathogenic mutations have been identified, which cause a range of  
712 metabolic, neuromuscular and developmental diseases. The vast majority of them can be  
713 explained because they affect key structural and functional features of mitochondrial  
714 carriers. Some of them are found in loop regions, which have not been included in this  
715 analysis, and others in extra domains, such as the regulatory domain of the  
716 aspartate/glutamate carrier, which have been explained before (FIGURE 2C) (157). The few  
717 that are remaining, often involve mutations that introduce different properties from those  
718 of the original residue (e.g. p.Asp69Tyr in SLC25A1, p.Cys23Arg in SLC25A20, or p.Thr56Pro  
719 in SLC25A22), which could impair the structure and function, but also the biogenesis of the  
720 carrier. To understand these diseases, it is really important to discriminate between these  
721 different options, but the majority of these pathogenic mutations have not been studied  
722 experimentally. Given the fact that so many amino acid residues are important for the  
723 function of mitochondrial carriers, and that the SLC25 family is the largest solute carrier  
724 family in humans, it is likely that many more disease variants will be discovered.

725

726 **Acknowledgments**

727 Edmund Kunji, Martin King and Jonathan Ruprecht would like to thank the Medical Research  
728 Council UK for funding (programme grant MC\_UU\_00015/1). Chancievan Thangaratnarajah  
729 received funding from the European Union's Horizon 2020 research and innovation  
730 programme under the Marie Skłodowska-Curie grant agreement No. 847675.

731

732 **References**

- 733 1. Abrams AJ, Fontanesi F, Tan NBL, Buglo E, Campeanu IJ, Rebelo AP, Kornberg AJ,  
734 Phelan DG, Stark Z, and Zuchner S. Insights into the genotype-phenotype correlation  
735 and molecular function of SLC25A46. *Hum Mutat* 39: 1995-2007, 2018.  
736 doi:10.1002/humu.23639.
- 737 2. Abrams AJ, Hufnagel RB, Rebelo A, Zanna C, Patel N, Gonzalez MA, Campeanu IJ, Griffin  
738 LB, Groenewald S, Strickland AV, Tao F, Speziani F, Abreu L, Schule R, Caporali L, La  
739 Morgia C, Maresca A, Liguori R, Lodi R, Ahmed ZM, Sund KL, Wang X, Krueger LA, Peng  
740 Y, Prada CE, Prows CA, Schorry EK, Antonellis A, Zimmerman HH, Abdul-Rahman OA,  
741 Yang Y, Downes SM, Prince J, Fontanesi F, Barrientos A, Nemeth AH, Carelli V, Huang T,  
742 Zuchner S, and Dallman JE. Mutations in SLC25A46, encoding a UGO1-like protein,  
743 cause an optic atrophy spectrum disorder. *Nat Genet* 47: 926-932, 2015.  
744 doi:10.1038/ng.3354.
- 745 3. Agrimi G, Di Noia MA, Marobbio CM, Fiermonte G, Lasorsa FM, and Palmieri F.  
746 Identification of the human mitochondrial S-adenosylmethionine transporter: bacterial  
747 expression, reconstitution, functional characterization and tissue distribution. *Biochem*  
748 *J* 379: 183-190, 2004.
- 749 4. Almannai M, Alasmari A, Alqasmi A, Faqeih E, Al Mutairi F, Alotaibi M, Samman MM,  
750 Eyaid W, Aljadhari YI, Shamseldin HE, Craigen W, and Alkuraya FS. Expanding the  
751 phenotype of SLC25A42-associated mitochondrial encephalomyopathy. *Clin Genet* 93:  
752 1097-1102, 2018. doi:10.1111/cge.13210.
- 753 5. Aprille JR. Mechanism and regulation of the mitochondrial ATP-Mg/P(i) carrier. *J*  
754 *Bioenerg Biomembr* 25: 473-481, 1993. doi:10.1007/bf01108404.

- 755 6. Aquila H, Link TA, and Klingenberg M. The uncoupling protein from brown fat  
756 mitochondria is related to the mitochondrial ADP/ATP carrier. *EMBO J* 4: 2369-2376,  
757 1985.
- 758 7. Aquila H, Misra D, Eulitz M, and Klingenberg M. Complete amino acid sequence of the  
759 ADP/ATP carrier from beef heart mitochondria. *Hoppe Seylers Z Physiol Chem* 363:  
760 345-349, 1982.
- 761 8. Austin J, and Aprille JR. Carboxyatractyloside-insensitive influx and efflux of adenine  
762 nucleotides in rat liver mitochondria. *J Biol Chem* 259: 154-160, 1984.
- 763 9. Azzi A, Chappell JB, and Robinson BH. Penetration of the mitochondrial membrane by  
764 glutamate and aspartate. *Biochem Biophys Res Commun* 29: 148-152, 1967. doi:0006-  
765 291X(67)90556-6.
- 766 10. Bamber L, Harding M, Butler PJG, and Kunji ERS. Yeast mitochondrial ADP/ATP carriers  
767 are monomeric in detergents. *Proc Natl Acad Sci USA* 103: 16224-16229, 2006. doi:Doi  
768 10.1073/Pnas.0607640103.
- 769 11. Bamber L, Harding M, Monné M, Slotboom DJ, and Kunji ERS. The yeast mitochondrial  
770 ADP/ATP carrier functions as a monomer in mitochondrial membranes. *Proc Natl Acad*  
771 *Sci USA* 104: 10830-10834, 2007. doi:doi.org/10.1073/pnas.0703969104.
- 772 12. Bamber L, Slotboom DJ, and Kunji ERS. Yeast mitochondrial ADP/ATP carriers are  
773 monomeric in detergents as demonstrated by differential affinity purification. *J Mol*  
774 *Biol* 371: 388-395, 2007. doi:10.1016/j.jmb.2007.05.072.
- 775 13. Bertholet AM, Chouchani ET, Kazak L, Angelin A, Fedorenko A, Long JZ, Vidoni S, Garrity  
776 R, Cho J, Terada N, Wallace DC, Spiegelman BM, and Kirichok Y. H(+) transport is an  
777 integral function of the mitochondrial ADP/ATP carrier. *Nature* 571: 515-520, 2019.  
778 doi:10.1038/s41586-019-1400-3.
- 779 14. Beyer K, and Klingenberg M. ADP/ATP carrier protein from beef heart mitochondria  
780 has high amounts of tightly bound cardiolipin, as revealed by <sup>31</sup>P nuclear magnetic  
781 resonance. *Biochemistry* 24: 3821-3826, 1985.
- 782 15. Bhoj EJ, Li M, Ahrens-Nicklas R, Pyle LC, Wang J, Zhang VW, Clarke C, Wong LJ,  
783 Sondheimer N, Ficicioglu C, and Yudkoff M. Pathologic variants of the mitochondrial  
784 phosphate carrier SLC25A3: two new patients and expansion of the  
785 cardiomyopathy/skeletal myopathy phenotype with and without lactic acidosis. *JIMD*  
786 *reports* 19: 59-66, 2015. doi:10.1007/8904\_2014\_364.

- 787 16. Bisaccia F, De Palma A, and Palmieri F. Identification and purification of the  
788 aspartate/glutamate carrier from bovine heart mitochondria. *Biochim Biophys Acta*  
789 1106: 291-296, 1992.
- 790 17. Boczonadi V, King MS, Smith AC, Olahova M, Bansagi B, Roos A, Eyassu F, Borchers C,  
791 Ramesh V, Lochmuller H, Polvikoski T, Whittaker RG, Pyle A, Griffin H, Taylor RW,  
792 Chinnery PF, Robinson AJ, Kunji ERS, and Horvath R. Mitochondrial oxodicarboxylate  
793 carrier deficiency is associated with mitochondrial DNA depletion and spinal muscular  
794 atrophy-like disease. *Genet Med* 2018. doi:10.1038/gim.2017.251.
- 795 18. Brand MD, and Chappell JB. Glutamate and aspartate transport in rat brain  
796 mitochondria. *Biochem J* 140: 205-210, 1974.
- 797 19. Bricker DK, Taylor EB, Schell JC, Orsak T, Boutron A, Chen YC, Cox JE, Cardon CM, Van  
798 Vranken JG, Dephoure N, Redin C, Boudina S, Gygi SP, Brivet M, Thummel CS, and  
799 Rutter J. A mitochondrial pyruvate carrier required for pyruvate uptake in yeast,  
800 *Drosophila*, and humans. *Science* 337: 96-100, 2012. doi:10.1126/science.1218099.
- 801 20. Brustovetsky N, and Klingenberg M. The reconstituted ADP/ATP carrier can mediate H<sup>+</sup>  
802 transport by free fatty acids, which is further stimulated by mersalyl. *J Biol Chem* 269:  
803 27329-27336, 1994.
- 804 21. Buffet A, Morin A, Castro-Vega LJ, Habarou F, Lussey-Lepoutre C, Letouze E, Lefebvre  
805 H, Guilhem I, Haissaguerre M, Raingeard I, Padilla-Girola M, Tran T, Tchara L, Bertherat  
806 J, Amar L, Ottolenghi C, Burnichon N, Gimenez-Roqueplo AP, and Favier J. Germline  
807 mutations in the mitochondrial 2-oxoglutarate/malate carrier SLC25A11 gene confer a  
808 predisposition to metastatic paragangliomas. *Cancer Res* 78: 1914-1922, 2018.  
809 doi:10.1158/0008-5472.CAN-17-2463.
- 810 22. Camacho JA, Obie C, Biery B, Goodman BK, Hu CA, Almashanu S, Steel G, Casey R,  
811 Lambert M, Mitchell GA, and Valle D. Hyperornithinaemia-hyperammonaemia-  
812 homocitrullinuria syndrome is caused by mutations in a gene encoding a mitochondrial  
813 ornithine transporter. *Nat Genet* 22: 151-158, 1999.
- 814 23. Cannon B, and Nedergaard J. What Ignites UCP1? *Cell metabolism* 26: 697-698, 2017.  
815 doi:10.1016/j.cmet.2017.10.012.
- 816 24. Cappello AR, Curcio R, Valeria Miniero D, Stipani I, Robinson AJ, Kunji ERS, and Palmieri  
817 F. Functional and structural role of amino acid residues in the even-numbered

- 818 transmembrane alpha-helices of the bovine mitochondrial oxoglutarate carrier. *J Mol*  
819 *Biol* 363: 51-62, 2006.
- 820 25. Cappello AR, Miniero DV, Curcio R, Ludovico A, Daddabbo L, Stipani I, Robinson AJ,  
821 Kunji ERS, and Palmieri F. Functional and structural role of amino acid residues in the  
822 odd-numbered transmembrane alpha-helices of the bovine mitochondrial oxoglutarate  
823 carrier. *J Mol Biol* 369: 400-412, 2007.
- 824 26. Cavero S, Traba J, Del Arco A, and Satrustegui J. The calcium-dependent ATP-Mg/Pi  
825 mitochondrial carrier is a target of glucose-induced calcium signalling in  
826 *Saccharomyces cerevisiae*. *Biochem J* 392: 537-544, 2005.
- 827 27. Chaouch A, Porcelli V, Cox D, Edvardson S, Scarcia P, De Grassi A, Pierri CL, Cossins J,  
828 Laval SH, Griffin H, Muller JS, Evangelista T, Topf A, Abicht A, Huebner A, von der  
829 Hagen M, Bushby K, Straub V, Horvath R, Elpeleg O, Palace J, Senderek J, Beeson D,  
830 Palmieri L, and Lochmuller H. Mutations in the mitochondrial citrate carrier SLC25A1  
831 are associated with impaired neuromuscular transmission. *J Neuromuscul Dis* 1: 75-90,  
832 2014. doi:10.3233/JND-140021.
- 833 28. Chorev DS, Baker LA, Wu D, Beilsten-Edmands V, Rouse SL, Zeev-Ben-Mordehai T, Jiko  
834 C, Samsudin F, Gerle C, Khalid S, Stewart AG, Matthews SJ, Grunewald K, and Robinson  
835 CV. Protein assemblies ejected directly from native membranes yield complexes for  
836 mass spectrometry. *Science* 362: 829-834, 2018. doi:10.1126/science.aau0976.
- 837 29. Chung J, Anderson SA, Gwynn B, Deck KM, Chen MJ, Langer NB, Shaw GC, Huston NC,  
838 Boyer LF, Datta S, Paradkar PN, Li L, Wei Z, Lambert AJ, Sahr K, Wittig JG, Chen W, Lu  
839 W, Galy B, Schlaeger TM, Hentze MW, Ward DM, Kaplan J, Eisenstein RS, Peters LL, and  
840 Paw BH. Iron regulatory protein-1 protects against mitoferrin-1-deficient porphyria. *J*  
841 *Biol Chem* 289: 7835-7843, 2014. doi:10.1074/jbc.M114.547778.
- 842 30. Cohen I, Staretz-Chacham O, Wormser O, Perez Y, Saada A, Kadir R, and Birk OS. A  
843 novel homozygous SLC25A1 mutation with impaired mitochondrial complex V: Possible  
844 phenotypic expansion. *Am J Med Genet Part A* 176: 330-336, 2018.  
845 doi:10.1002/ajmg.a.38574.
- 846 31. Cozens AL, Runswick MJ, and Walker JE. DNA sequences of two expressed nuclear  
847 genes for human mitochondrial ADP/ATP translocase. *J Mol Biol* 206: 261-280, 1989.  
848 doi:10.1016/0022-2836(89)90477-4.

- 849 32. Crichton PG, Harding M, Ruprecht JJ, Lee Y, and Kunji ERS. Lipid, detergent, and  
850 Coomassie Blue G-250 affect the migration of small membrane proteins in blue native  
851 gels; mitochondrial carriers migrate as monomers not dimers. *J Biol Chem* 288: 22163-  
852 22173, 2013. doi:Doi 10.1074/Jbc.M113.484329.
- 853 33. Crichton PG, Lee Y, and Kunji ERS. The molecular features of uncoupling protein 1  
854 support a conventional mitochondrial carrier-like mechanism. *Biochimie* 134: 35-50,  
855 2017. doi:10.1016/j.biochi.2016.12.016.
- 856 34. Crichton PG, Lee Y, Ruprecht JJ, Cerson E, Thangaratnarajah C, King MS, and Kunji ERS.  
857 Trends in thermostability provide information on the nature of substrate, inhibitor,  
858 and lipid interactions with mitochondrial carriers. *J Biol Chem* 290: 8206-8217, 2015.  
859 doi:10.1074/jbc.M114.616607.
- 860 35. Dehez F, Pebay-Peyroula E, and Chipot C. Binding of ADP in the mitochondrial ADP/ATP  
861 carrier is driven by an electrostatic funnel. *J Am Chem Soc* 130: 12725-12733, 2008.
- 862 36. del Arco A, and Satrustegui J. Identification of a novel human subfamily of  
863 mitochondrial carriers with calcium-binding domains. *J Biol Chem* 279: 24701-24713,  
864 2004. doi:10.1074/jbc.M401417200.
- 865 37. Di Noia MA, Todisco S, Cirigliano A, Rinaldi T, Agrimi G, Iacobazzi V, and Palmieri F. The  
866 human SLC25A33 and SLC25A36 genes of solute carrier family 25 encode two  
867 mitochondrial pyrimidine nucleotide transporters. *J Biol Chem* 289: 33137-33148,  
868 2014. doi:10.1074/jbc.M114.610808.
- 869 38. Dimmock D, Maranda B, Dionisi-Vici C, Wang J, Kleppe S, Fiermonte G, Bai R, Hainline  
870 B, Hamosh A, O'Brien WE, Scaglia F, and Wong LJ. Citrin deficiency, a perplexing global  
871 disorder. *Mol Genet Metab* 96: 44-49, 2009. doi:10.1016/j.ymgme.2008.10.007.
- 872 39. Dolce V, Fiermonte G, Runswick MJ, Palmieri F, and Walker JE. The human  
873 mitochondrial deoxynucleotide carrier and its role in the toxicity of nucleoside  
874 antivirals. *Proc Natl Acad Sci USA* 98: 2284-2288, 2001.
- 875 40. Dolce V, Scarcia P, Iacopetta D, and Palmieri F. A fourth ADP/ATP carrier isoform in  
876 man: identification, bacterial expression, functional characterization and tissue  
877 distribution. *FEBS Lett* 579: 633-637, 2005.
- 878 41. Duncan AL, Ruprecht JJ, Kunji ERS, and Robinson AJ. Cardiolipin dynamics and binding  
879 to conserved residues in the mitochondrial ADP/ATP carrier. *Biochim Biophys Acta*  
880 1860: 1035-1045, 2018. doi:10.1016/j.bbamem.2018.01.017.



- 881 42. Edvardson S, Porcelli V, J alas C, Soiferman D, Kellner Y, Shaag A, Korman SH, Pi erri CL,  
882 Scarcia P, Fraenkel ND, Segel R, Schechter A, Frumkin A, Pines O, Saada A, Palmieri L,  
883 and Elpeleg O. Agenesis of corpus callosum and optic nerve hypoplasia due to  
884 mutations in SLC25A1 encoding the mitochondrial citrate transporter. *Journal of*  
885 *medical genetics* 50: 240-245, 2013. doi:10.1136/jmedgenet-2012-101485.
- 886 43. Ehmke N, Graul-Neumann L, Smorag L, Koenig R, Segebrecht L, Magoulas P, Scaglia F,  
887 Kilic E, Hennig AF, Adolphs N, Saha N, Fauler B, Kalscheuer VM, Hennig F, Altmuller J,  
888 Netzer C, Thiele H, Nurnberg P, Yigit G, Jager M, Hecht J, Kruger U, Mielke T, Krawitz  
889 PM, Horn D, Schuelke M, Mundlos S, Bacino CA, Bonnen PE, Wollnik B, Fischer-Zirnsak  
890 B, and Kornak U. De novo mutations in SLC25A24 cause a craniosynostosis syndrome  
891 with hypertrichosis, progeroid appearance, and mitochondrial dysfunction. *Am J Hum*  
892 *Genet* 101: 833-843, 2017. doi:10.1016/j.ajhg.2017.09.016.
- 893 44. Fedorenko A, Lishko PV, and Kirichok Y. Mechanism of fatty-acid-dependent UCP1  
894 uncoupling in brown fat mitochondria. *Cell* 151: 400-413, 2012.  
895 doi:10.1016/j.cell.2012.09.010.
- 896 45. Fiermonte G, De Leonardis F, Todisco S, Palmieri L, Lasorsa FM, and Palmieri F.  
897 Identification of the mitochondrial ATP-Mg/Pi transporter. Bacterial expression,  
898 reconstitution, functional characterization, and tissue distribution. *J Biol Chem* 279:  
899 30722-30730, 2004.
- 900 46. Fiermonte G, Dolce V, Arrigoni R, Runswick MJ, Walker JE, and Palmieri F. Organization  
901 and sequence of the gene for the human mitochondrial dicarboxylate carrier:  
902 evolution of the carrier family. *Biochem J* 344: 953-960, 1999.
- 903 47. Fiermonte G, Dolce V, David L, Santorelli FM, Dionisi-Vici C, Palmieri F, and Walker JE.  
904 The mitochondrial ornithine transporter. Bacterial expression, reconstitution,  
905 functional characterization, and tissue distribution of two human isoforms. *J Biol Chem*  
906 278: 32778-32783, 2003.
- 907 48. Fiermonte G, Dolce V, Palmieri L, Ventura M, Runswick MJ, Palmieri F, and Walker JE.  
908 Identification of the human mitochondrial oxodicarboxylate carrier. Bacterial  
909 expression, reconstitution, functional characterization, tissue distribution, and  
910 chromosomal location. *J Biol Chem* 276: 8225-8230, 2001.
- 911 49. Fiermonte G, Palmieri L, Dolce V, Lasorsa FM, Palmieri F, Runswick MJ, and Walker JE.  
912 The sequence, bacterial expression, and functional reconstitution of the rat

- 913 mitochondrial dicarboxylate transporter cloned via distant homologs in yeast and  
914 *Caenorhabditis elegans*. *J Biol Chem* 273: 24754-24759, 1998.
- 915 50. Fiermonte G, Palmieri L, Todisco S, Agrimi G, Palmieri F, and Walker JE. Identification of  
916 the mitochondrial glutamate transporter. Bacterial expression, reconstitution,  
917 functional characterization, and tissue distribution of two human isoforms. *J Biol Chem*  
918 277: 19289-19294, 2002.
- 919 51. Fiermonte G, Paradies E, Todisco S, Marobbio CM, and Palmieri F. A novel member of  
920 solute carrier family 25 (SLC25A42) is a transporter of coenzyme A and adenosine 3',5'-  
921 diphosphate in human mitochondria. *J Biol Chem* 284: 18152-18159, 2009.  
922 doi:10.1074/jbc.M109.014118.
- 923 52. Floyd S, Favre C, Lasorsa FM, Leahy M, Trigiante G, Stroebel P, Marx A, Loughran G,  
924 O'Callaghan K, Marobbio CM, Slotboom DJ, Kunji ERS, Palmieri F, and O'Connor R. The  
925 insulin-like growth factor-I-mTOR signaling pathway induces the mitochondrial  
926 pyrimidine nucleotide carrier to promote cell growth. *Mol Biol Cell* 18: 3545-3555,  
927 2007. doi:10.1091/mbc.e06-12-1109.
- 928 53. Fontanesi F, Palmieri L, Scarcia P, Lodi T, Donnini C, Limongelli A, Tiranti V, Zeviani M,  
929 Ferrero I, and Viola AM. Mutations in AAC2, equivalent to human adPEO-associated  
930 ANT1 mutations, lead to defective oxidative phosphorylation in *Saccharomyces*  
931 *cerevisiae* and affect mitochondrial DNA stability. *Hum Mol Genet* 13: 923-934, 2004.  
932 doi:10.1093/hmg/ddh108.
- 933 54. Gorgoglione R, Porcelli V, Santoro A, Daddabbo L, Voza A, Monne M, Di Noia MA,  
934 Palmieri L, Fiermonte G, and Palmieri F. The human uncoupling proteins 5 and 6  
935 (UCP5/SLC25A14 and UCP6/SLC25A30) transport sulfur oxyanions, phosphate and  
936 dicarboxylates. *Biochim Biophys Acta Bioenerg* 1860: 724-733, 2019.  
937 doi:10.1016/j.bbabi.2019.07.010.
- 938 55. Goubert E, Mircheva Y, Lasorsa FM, Melon C, Profilo E, Sutera J, Becq H, Palmieri F,  
939 Palmieri L, Aniksztejn L, and Molinari F. Inhibition of the mitochondrial glutamate  
940 carrier SLC25A22 in astrocytes leads to intracellular glutamate accumulation. *Front Cell*  
941 *Neurosci* 11: 149, 2017. doi:10.3389/fncel.2017.00149.
- 942 56. Haghghi A, Haack TB, Atiq M, Mottaghi H, Haghghi-Kakhki H, Bashir RA, Ahting U,  
943 Feichtinger RG, Mayr JA, Rotig A, Lebre AS, Klopstock T, Dworschak A, Pulido N, Saeed  
944 MA, Saleh-Gohari N, Holzerova E, Chinnery PF, Taylor RW, and Prokisch H. Sengers

- 945 syndrome: six novel AGK mutations in seven new families and review of the  
946 phenotypic and mutational spectrum of 29 patients. *Orphanet J Rare Dis* 9: 119, 2014.  
947 doi:10.1186/s13023-014-0119-3.
- 948 57. Haitina T, Lindblom J, Renstrom T, and Fredriksson R. Fourteen novel human members  
949 of mitochondrial solute carrier family 25 (SLC25) widely expressed in the central  
950 nervous system. *Genomics* 88: 779-790, 2006.
- 951 58. Harborne SP, King MS, Crichton PG, and Kunji ERS. Calcium regulation of the human  
952 mitochondrial ATP-Mg/Pi carrier SLC25A24 uses a locking pin mechanism. *Sci Rep* 7:  
953 45383, 2017. doi:10.1038/srep45383.
- 954 59. Harborne SP, Ruprecht JJ, and Kunji ERS. Calcium-induced conformational changes in  
955 the regulatory domain of the human mitochondrial ATP-Mg/Pi carrier. *Biochim Biophys*  
956 *Acta* 1847: 1245-1253, 2015. doi:10.1016/j.bbabi.2015.07.002.
- 957 60. Harborne SPD, and Kunji ERS. Calcium-regulated mitochondrial ATP-Mg/Pi carriers  
958 evolved from a fusion of an EF-hand regulatory domain with a mitochondrial ADP/ATP  
959 carrier-like domain. *IUBMB life* 70: 1222-1232, 2018. doi:10.1002/iub.1931.
- 960 61. Herzig S, Raemy E, Montessuit S, Veuthey JL, Zamboni N, Westermann B, Kunji ERS,  
961 and Martinou JC. Identification and functional expression of the mitochondrial  
962 pyruvate carrier. *Science* 337: 93-96, 2012. doi:10.1126/science.1218530.
- 963 62. Hirst J, Kunji ERS, and Walker JE. Comment on "Protein assemblies ejected directly  
964 from native membranes yield complexes for mass spectrometry". *Science* 366: 2019.  
965 doi:10.1126/science.aaw9830.
- 966 63. Hoffmann B, Stockl A, Schlame M, Beyer K, and Klingenberg M. The reconstituted  
967 ADP/ATP carrier activity has an absolute requirement for cardiolipin as shown in  
968 cysteine mutants. *J Biol Chem* 269: 1940-1944, 1994.
- 969 64. Hofherr A, Seger C, Fitzpatrick F, Busch T, Michel E, Luan J, Osterried L, Linden F,  
970 Kramer-Zucker A, Wakimoto B, Schutze C, Wiedemann N, Artati A, Adamski J, Walz G,  
971 Kunji ERS, Montell C, Watnick T, and Kottgen M. The mitochondrial transporter  
972 SLC25A25 links ciliary TRPP2 signaling and cellular metabolism. *PLoS Biol* 16: e2005651,  
973 2018. doi:10.1371/journal.pbio.2005651.
- 974 65. Hommes FA, Roesel RA, Metoki K, Hartlage PL, and Dyken PR. Studies on a case of  
975 HHH-syndrome (hyperammonemia, hyperornithinemia, homocitrullinuria).  
976 *Neuropediatrics* 17: 48-52, 1986. doi:10.1055/s-2008-1052499.

- 977 66. Huizing M, Iacobazzi V, Ijlst L, Savelkoul P, Ruitenbeek W, van den Heuvel L, Indiveri C,  
978 Smeitink J, Trijbels F, Wanders R, and Palmieri F. Cloning of the human carnitine-  
979 acylcarnitine carrier cDNA and identification of the molecular defect in a patient. *Am J*  
980 *Hum Genet* 61: 1239-1245, 1997.
- 981 67. Huizing M, Ruitenbeek W, van den Heuvel LP, Dolce V, Iacobazzi V, Smeitink JA,  
982 Palmieri F, and Trijbels JM. Human mitochondrial transmembrane metabolite carriers:  
983 tissue distribution and its implication for mitochondrial disorders. *J Bioenerg Biomembr*  
984 30: 277-284, 1998.
- 985 68. Iacobazzi V, Lauria G, and Palmieri F. Organization and sequence of the human gene  
986 for the mitochondrial citrate transport protein. *DNA Seq* 7: 127-139, 1997.
- 987 69. Iacobazzi V, Palmieri F, Runswick MJ, and Walker JE. Sequences of the human and  
988 bovine genes for the mitochondrial 2-oxoglutarate carrier. *DNA Seq* 3: 79-88, 1992.
- 989 70. Indiveri C, Tonazzi A, and Palmieri F. Identification and purification of the carnitine  
990 carrier from rat liver mitochondria. *Biochim Biophys Acta* 1020: 81-86, 1990.
- 991 71. Janer A, Prudent J, Paupe V, Fahiminiya S, Majewski J, Sgarioto N, Des Rosiers C, Forest  
992 A, Lin ZY, Gingras AC, Mitchell G, McBride HM, and Shoubridge EA. SLC25A46 is  
993 required for mitochondrial lipid homeostasis and cristae maintenance and is  
994 responsible for Leigh syndrome. *EMBO Mol Med* 8: 1019-1038, 2016.  
995 doi:10.15252/emmm.201506159.
- 996 72. Jezek P, Jaburek M, and Garlid KD. Channel character of uncoupling protein-mediated  
997 transport. *FEBS Lett* 584: 2135-2141, 2010. doi:S0014-5793(10)00172-9 [pii]  
998 10.1016/j.febslet.2010.02.068.
- 999 73. Johnson RN, and Chappell JB. The transport of inorganic phosphate by the  
1000 mitochondrial dicarboxylate carrier. *Biochem J* 134: 769-774, 1973.
- 1001 74. Jordens EZ, Palmieri L, Huizing M, van den Heuvel LP, Sengers RC, Dorner A,  
1002 Ruitenbeek W, Trijbels FJ, Valsson J, Sigfusson G, Palmieri F, and Smeitink JA. Adenine  
1003 nucleotide translocator 1 deficiency associated with Sengers syndrome. *Annals of*  
1004 *neurology* 52: 95-99, 2002.
- 1005 75. Kadenbach B, Mende P, Kolbe HV, Stipani I, and Palmieri F. The mitochondrial  
1006 phosphate carrier has an essential requirement for cardiolipin. *FEBS Lett* 139: 109-112,  
1007 1982.

- 1008 76. Kaplan RS, Mayor JA, Johnston N, and Oliveira DL. Purification and characterization of  
1009 the reconstitutively active tricarboxylate transporter from rat liver mitochondria. *J Biol*  
1010 *Chem* 265: 13379-13385, 1990.
- 1011 77. Kaukonen J, Juselius JK, Tiranti V, Kyttala A, Zeviani M, Comi GP, Keranen S, Peltonen L,  
1012 and Suomalainen A. Role of adenine nucleotide translocator 1 in mtDNA maintenance.  
1013 *Science* 289: 782-785, 2000.
- 1014 78. Kelley RI, Robinson D, Puffenberger EG, Strauss KA, and Morton DH. Amish lethal  
1015 microcephaly: a new metabolic disorder with severe congenital microcephaly and 2-  
1016 ketoglutaric aciduria. *Am J Med Genet* 112: 318-326, 2002. doi:10.1002/ajmg.10529.
- 1017 79. Khan S, Ansar M, Khan AK, Shah K, Muhammad N, Shahzad S, Nickerson DA, Bamshad  
1018 MJ, Santos-Cortez RLP, Leal SM, and Ahmad W. A homozygous missense mutation in  
1019 SLC25A16 associated with autosomal recessive isolated fingernail dysplasia in a  
1020 Pakistani family. *Br J Dermatol* 178: 556-558, 2018. doi:10.1111/bjd.15661.
- 1021 80. King MS, Kerr M, Crichton PG, Springett R, and Kunji ERS. Formation of a cytoplasmic  
1022 salt bridge network in the matrix state is a fundamental step in the transport  
1023 mechanism of the mitochondrial ADP/ATP carrier. *Biochim Biophys Acta* 1857: 14-22,  
1024 2016. doi:10.1016/j.bbabi.2015.09.013.
- 1025 81. King MS, Thompson K, Hopton S, He L, Kunji ERS, Taylor RW, and Ortiz-Gonzalez XR.  
1026 Expanding the phenotype of de novo SLC25A4-linked mitochondrial disease to include  
1027 mild myopathy. *Neurol Genet* 4: e256, 2018. doi:10.1212/NXG.0000000000000256.
- 1028 82. Kishita Y, Pajak A, Bolar NA, Marobbio CM, Maffezzini C, Miniero DV, Monne M, Kohda  
1029 M, Stranneheim H, Murayama K, Naess K, Lesko N, Bruhn H, Mourier A, Wibom R,  
1030 Nennesmo I, Jespers A, Govaert P, Ohtake A, Van Laer L, Loeys BL, Freyer C, Palmieri F,  
1031 Wredenberg A, Okazaki Y, and Wedell A. Intra-mitochondrial Methylation Deficiency  
1032 Due to Mutations in SLC25A26. *Am J Hum Genet* 97: 761-768, 2015.  
1033 doi:10.1016/j.ajhg.2015.09.013.
- 1034 83. Klingenberg M. The ADP and ATP transport in mitochondria and its carrier. *Biochim*  
1035 *Biophys Acta* 1778: 1978-2021, 2008.
- 1036 84. Klingenberg M. UCP1 - A sophisticated energy valve. *Biochimie* 134: 19-27, 2017.  
1037 doi:10.1016/j.biochi.2016.10.012.

- 1038 85. Knight SAB, Yoon H, Pandey AK, Pain J, Pain D, and Dancis A. Splitting the functions of  
1039 Rim2, a mitochondrial iron/pyrimidine carrier. *Mitochondrion* 47: 256-265, 2019.  
1040 doi:10.1016/j.mito.2018.12.005.
- 1041 86. Kobayashi K, Sinasac DS, Iijima M, Boright AP, Begum L, Lee JR, Yasuda T, Ikeda S,  
1042 Hirano R, Terazono H, Crackower MA, Kondo I, Tsui LC, Scherer SW, and Saheki T. The  
1043 gene mutated in adult-onset type II citrullinaemia encodes a putative mitochondrial  
1044 carrier protein. *Nat Genet* 22: 159-163, 1999.
- 1045 87. Kory N, Wyant GA, Prakash G, Uit de Bos J, Bottanelli F, Pacold ME, Chan SH, Lewis CA,  
1046 Wang T, Keys HR, Guo YE, and Sabatini DM. SFXN1 is a mitochondrial serine  
1047 transporter required for one-carbon metabolism. *Science* 362: 2018.  
1048 doi:10.1126/science.aat9528.
- 1049 88. Ku DH, Kagan J, Chen ST, Chang CD, Baserga R, and Wurzel J. The human fibroblast  
1050 adenine nucleotide translocator gene. Molecular cloning and sequence. *J Biol Chem*  
1051 265: 16060-16063, 1990.
- 1052 89. Kunji ERS. *Structural and Mechanistic Aspects of Mitochondrial Transport Proteins*.  
1053 Elsevier, 2012, p. 174–205.
- 1054 90. Kunji ERS, Aleksandrova A, King MS, Majd H, Ashton VL, Cerson E, Springett R,  
1055 Kibalchenko M, Tavoulari S, Crichton PG, and Ruprecht JJ. The transport mechanism of  
1056 the mitochondrial ADP/ATP carrier. *Biochim Biophys Acta* 1863: 2379-2393, 2016.  
1057 doi:10.1016/j.bbamcr.2016.03.015.
- 1058 91. Kunji ERS, and Crichton PG. Mitochondrial carriers function as monomers. *Biochim*  
1059 *Biophys Acta* 1797: 817-831, 2010. doi:10.1016/j.bbabbio.2010.03.023.
- 1060 92. Kunji ERS, and Harding M. Projection structure of the atractyloside-inhibited  
1061 mitochondrial ADP/ATP carrier of *Saccharomyces cerevisiae*. *J Biol Chem* 278: 36985-  
1062 36988, 2003.
- 1063 93. Kunji ERS, Harding M, Butler PJG, and Akamine P. Determination of the molecular mass  
1064 and dimensions of membrane proteins by size exclusion chromatography. *Methods* 46:  
1065 62-72, 2008. doi:10.1016/j.jymeth.2008.10.020.
- 1066 94. Kunji ERS, and Robinson AJ. The conserved substrate binding site of mitochondrial  
1067 carriers. *Biochim Biophys Acta* 1757: 1237-1248, 2006.  
1068 doi:10.1016/j.bbabbio.2006.03.021.

- 1069 95. Kunji ERS, and Robinson AJ. Coupling of proton and substrate translocation in the  
1070 transport cycle of mitochondrial carriers. *Curr Opin Struct Biol* 20: 440-447, 2010.  
1071 doi:10.1016/j.sbi.2010.06.004.
- 1072 96. Lee Y, Willers C, Kunji ERS, and Crichton PG. Uncoupling protein 1 binds one nucleotide  
1073 per monomer and is stabilized by tightly bound cardiolipin. *Proc Natl Acad Sci U S A*  
1074 112: 6973-6978, 2015. doi:10.1073/pnas.1503833112.
- 1075 97. Lemattre C, Imbert-Bouteille M, Gatinois V, Benit P, Sanchez E, Guignard T, Tran Mau-  
1076 Them F, Haquet E, Rivier F, Carme E, Roubertie A, Boland A, Lechner D, Meyer V,  
1077 Thevenon J, Duffourd Y, Riviere JB, Deleuze JF, Wells C, Molinari F, Rustin P, Blanchet P,  
1078 and Genevieve D. Report on three additional patients and genotype-phenotype  
1079 correlation in SLC25A22-related disorders group. *Eur J Hum Genet* 27: 1692-1700,  
1080 2019. doi:10.1038/s41431-019-0433-2.
- 1081 98. Lill R, and Kispal G. Mitochondrial ABC transporters. *Res Microbiol* 152: 331-340, 2001.
- 1082 99. Lindhurst MJ, Fiermonte G, Song S, Struys E, De Leonardis F, Schwartzberg PL, Chen A,  
1083 Castegna A, Verhoeven N, Mathews CK, Palmieri F, and Biesecker LG. Knockout of  
1084 Slc25a19 causes mitochondrial thiamine pyrophosphate depletion, embryonic  
1085 lethality, CNS malformations, and anemia. *Proc Natl Acad Sci USA* 103: 15927-15932,  
1086 2006.
- 1087 100. Liu Y, Wang X, and Chen XJ. Misfolding of mutant adenine nucleotide translocase in  
1088 yeast supports a novel mechanism of Ant1-induced muscle diseases. *Mol Biol Cell* 26:  
1089 1985-1994, 2015. doi:10.1091/mbc.E15-01-0030.
- 1090 101. Liu Y, Wang X, Coyne LP, Yang Y, Qi Y, Middleton FA, and Chen XJ. Mitochondrial carrier  
1091 protein overloading and misfolding induce aggresomes and proteostatic adaptations in  
1092 the cytosol. *Mol Biol Cell* 30: 1272-1284, 2019. doi:10.1091/mbc.E19-01-0046.
- 1093 102. Lunetti P, Damiano F, De Benedetto G, Siculella L, Pennetta A, Muto L, Paradies E,  
1094 Marobbio CM, Dolce V, and Capobianco L. Characterization of human and yeast  
1095 mitochondrial glycine carriers with implications for heme biosynthesis and anemia. *J*  
1096 *Biol Chem* 291: 19746-19759, 2016. doi:10.1074/jbc.M116.736876.
- 1097 103. Majd H, King MS, Smith AC, and Kunji ERS. Pathogenic mutations of the human  
1098 mitochondrial citrate carrier SLC25A1 lead to impaired citrate export required for lipid,  
1099 dolichol, ubiquinone and sterol synthesis. *Biochim Biophys Acta* 1859: 1-7, 2018.  
1100 doi:10.1016/j.bbabi.2017.10.002.

- 1101 104. Mayr JA, Haack TB, Graf E, Zimmermann FA, Wieland T, Haberberger B, Superti-Furga  
1102 A, Kirschner J, Steinmann B, Baumgartner MR, Moroni I, Lamantea E, Zeviani M,  
1103 Rodenburg RJ, Smeitink J, Strom TM, Meitinger T, Sperl W, and Prokisch H. Lack of the  
1104 mitochondrial protein acylglycerol kinase causes Sengers syndrome. *Am J Hum Genet*  
1105 90: 314-320, 2012. doi:10.1016/j.ajhg.2011.12.005.
- 1106 105. Mayr JA, Merkel O, Kohlwein SD, Gebhardt BR, Bohles H, Fotschl U, Koch J, Jaksch M,  
1107 Lochmuller H, Horvath R, Freisinger P, and Sperl W. Mitochondrial phosphate-carrier  
1108 deficiency: a novel disorder of oxidative phosphorylation. *Am J Hum Genet* 80: 478-  
1109 484, 2007. doi:10.1086/511788.
- 1110 106. Mayr JA, Zimmermann FA, Horvath R, Schneider HC, Schoser B, Holinski-Feder E,  
1111 Czermin B, Freisinger P, and Sperl W. Deficiency of the mitochondrial phosphate carrier  
1112 presenting as myopathy and cardiomyopathy in a family with three affected children.  
1113 *Neuromuscul Disord* 21: 803-808, 2011. doi:10.1016/j.nmd.2011.06.005.
- 1114 107. Mifsud J, Ravaud S, Krammer EM, Chipot C, Kunji ERS, Pebay-Peyroula E, and Dehez F.  
1115 The substrate specificity of the human ADP/ATP carrier AAC1. *Mol Membr Biol* 30: 160-  
1116 168, 2013. doi:Doi 10.3109/09687688.2012.745175.
- 1117 108. Miniero DV, Cappello AR, Curcio R, Ludovico A, Daddabbo L, Stipani I, Robinson AJ,  
1118 Kunji ERS, and Palmieri F. Functional and structural role of amino acid residues in the  
1119 matrix alpha-helices, termini and cytosolic loops of the bovine mitochondrial  
1120 oxoglutarate carrier. *Biochim Biophys Acta* 1807: 302-310, 2011.  
1121 doi:10.1016/j.bbabi.2010.12.005.
- 1122 109. Mizuarai S, Miki S, Araki H, Takahashi K, and Kotani H. Identification of dicarboxylate  
1123 carrier Slc25a10 as malate transporter in de novo fatty acid synthesis. *J Biol Chem* 280:  
1124 32434-32441, 2005.
- 1125 110. Molinari F, Kaminska A, Fiermonte G, Boddaert N, Raas-Rothschild A, Plouin P, Palmieri  
1126 L, Brunelle F, Palmieri F, Dulac O, Munnich A, and Colleaux L. Mutations in the  
1127 mitochondrial glutamate carrier SLC25A22 in neonatal epileptic encephalopathy with  
1128 suppression bursts. *Clin Genet* 76: 188-194, 2009. doi:10.1111/j.1399-  
1129 0004.2009.01236.x.
- 1130 111. Monné M, Miniero DV, Daddabbo L, Robinson AJ, Kunji ERS, and Palmieri F. Substrate  
1131 specificity of the two mitochondrial ornithine carriers can be swapped by single



- 1132 mutation in substrate binding site. *J Biol Chem* 287: 7925-7934, 2012. doi:10.1074/Jbc.M111.324855.
- 1133
- 1134 112. Morciano P, Carrisi C, Capobianco L, Mannini L, Burgio G, Cestra G, De Benedetto GE,  
1135 Corona DF, Musio A, and Cenci G. A conserved role for the mitochondrial citrate  
1136 transporter Sea/SLC25A1 in the maintenance of chromosome integrity. *Hum Mol*  
1137 *Genet* 18: 4180-4188, 2009. doi:10.1093/hmg/ddp370.
- 1138 113. Muhlenhoff U, Stadler JA, Richhardt N, Seubert A, Eickhorst T, Schweyen RJ, Lill R, and  
1139 Wiesenberger G. A specific role of the yeast mitochondrial carriers MRS3/4p in  
1140 mitochondrial iron acquisition under iron-limiting conditions. *J Biol Chem* 278: 40612-  
1141 40620, 2003.
- 1142 114. Muhlhausen C, Salomons GS, Lukacs Z, Struys EA, van der Knaap MS, Ullrich K, and  
1143 Santer R. Combined D2-/L2-hydroxyglutaric aciduria (SLC25A1 deficiency): clinical  
1144 course and effects of citrate treatment. *J Inherit Metab Dis* 37: 775-781, 2014.  
1145 doi:10.1007/s10545-014-9702-y.
- 1146 115. Neckelmann N, Li K, Wade RP, Shuster R, and Wallace DC. cDNA sequence of a human  
1147 skeletal muscle ADP/ATP translocator: lack of a leader peptide, divergence from a  
1148 fibroblast translocator cDNA, and coevolution with mitochondrial DNA genes. *Proc Natl*  
1149 *Acad Sci U S A* 84: 7580-7584, 1987. doi:10.1073/pnas.84.21.7580.
- 1150 116. Nedergaard J, Bengtsson T, and Cannon B. Unexpected evidence for active brown  
1151 adipose tissue in adult humans. *Am J Physiol Endocrinol Metab* 293: E444-452, 2007.  
1152 doi:10.1152/ajpendo.00691.2006.
- 1153 117. Nelson DR, Felix CM, and Swanson JM. Highly conserved charge-pair networks in the  
1154 mitochondrial carrier family. *J Mol Biol* 277: 285-308, 1998.
- 1155 118. Nicholls DG. The bioenergetics of brown adipose tissue mitochondria. *FEBS Lett* 61:  
1156 103-110, 1976.
- 1157 119. Nicholls DG. The hunt for the molecular mechanism of brown fat thermogenesis.  
1158 *Biochimie* 134: 9-18, 2017. doi:10.1016/j.biochi.2016.09.003.
- 1159 120. Nicholls DG, and Rial E. A history of the first uncoupling protein, UCP1. *J Bioenerg*  
1160 *Biomembr* 31: 399-406, 1999.
- 1161 121. Nota B, Struys EA, Pop A, Jansen EE, Fernandez Ojeda MR, Kanhai WA, Kranendijk M,  
1162 van Dooren SJ, Bevova MR, Sistermans EA, Nieuwint AW, Barth M, Ben-Omran T,  
1163 Hoffmann GF, de Lonlay P, McDonald MT, Meberg A, Muntau AC, Nuoffer JM, Parini R,

- 1164 Read MH, Renneberg A, Santer R, Strahleck T, van Schaftingen E, van der Knaap MS,  
1165 Jakobs C, and Salomons GS. Deficiency in SLC25A1, encoding the mitochondrial citrate  
1166 carrier, causes combined D-2- and L-2-hydroxyglutaric aciduria. *Am J Hum Genet* 92:  
1167 627-631, 2013. doi:10.1016/j.ajhg.2013.03.009.
- 1168 122. Okano Y, Ohura T, Sakamoto O, and Inui A. Current treatment for citrin deficiency  
1169 during NICCD and adaptation/compensation stages: Strategy to prevent CTLN2. *Mol*  
1170 *Genet Metab* 127: 175-183, 2019. doi:10.1016/j.ymgme.2019.06.004.
- 1171 123. Palmieri F, and Monne M. Discoveries, metabolic roles and diseases of mitochondrial  
1172 carriers: A review. *Biochim Biophys Acta* 1863: 2362-2378, 2016.  
1173 doi:10.1016/j.bbamcr.2016.03.007.
- 1174 124. Palmieri F, Scarcia P, and Monne M. Diseases Caused by Mutations in Mitochondrial  
1175 Carrier Genes SLC25: A Review. *Biomolecules* 10: 2020. doi:10.3390/biom10040655.
- 1176 125. Palmieri L, Alberio S, Pisano I, Lodi T, Meznaric-Petrusa M, Zidar J, Santoro A, Scarcia P,  
1177 Fontanesi F, Lamantea E, Ferrero I, and Zeviani M. Complete loss-of-function of the  
1178 heart/muscle-specific adenine nucleotide translocator is associated with mitochondrial  
1179 myopathy and cardiomyopathy. *Hum Mol Genet* 14: 3079-3088, 2005.  
1180 doi:10.1093/hmg/ddi341.
- 1181 126. Palmieri L, Pardo B, Lasorsa FM, del Arco A, Kobayashi K, Iijima M, Runswick MJ,  
1182 Walker JE, Saheki T, Satrustegui J, and Palmieri F. Citrin and aralar1 are Ca(2+)-  
1183 stimulated aspartate/glutamate transporters in mitochondria. *EMBO J* 20: 5060-5069,  
1184 2001.
- 1185 127. Paul BT, Tesfay L, Winkler CR, Torti FM, and Torti SV. Sideroflexin 4 affects Fe-S cluster  
1186 biogenesis, iron metabolism, mitochondrial respiration and heme biosynthetic  
1187 enzymes. *Sci Rep* 9: 19634, 2019. doi:10.1038/s41598-019-55907-z.
- 1188 128. Pebay-Peyroula E, Dahout-Gonzalez C, Kahn R, Trezeguet V, Lauquin GJ, and Brandolin  
1189 G. Structure of mitochondrial ADP/ATP carrier in complex with carboxyatractyloside.  
1190 *Nature* 426: 39-44, 2003.
- 1191 129. Poduri A, Heinzen EL, Chitsazzadeh V, Lasorsa FM, Elhosary PC, LaCoursiere CM, Martin  
1192 E, Yuskaitis CJ, Hill RS, Atabay KD, Barry B, Partlow JN, Bashiri FA, Zeidan RM, Elmalik  
1193 SA, Kabiraj MM, Kothare S, Stodberg T, McTague A, Kurian MA, Scheffer IE, Barkovich  
1194 AJ, Palmieri F, Salih MA, and Walsh CA. SLC25A22 is a novel gene for migrating partial  
1195 seizures in infancy. *Ann Neurol* 74: 873-882, 2013. doi:10.1002/ana.23998.

- 1196 130. Pop A, Williams M, Struys EA, Monne M, Jansen EEW, De Grassi A, Kanhai WA, Scarcia  
1197 P, Ojeda MRF, Porcelli V, van Dooren SJM, Lennertz P, Nota B, Abdenur JE, Coman D,  
1198 Das AM, El-Gharbawy A, Nuoffer JM, Polic B, Santer R, Weinhold N, Zuccarelli B,  
1199 Palmieri F, Palmieri L, and Salomons GS. An overview of combined D-2- and L-2-  
1200 hydroxyglutaric aciduria: functional analysis of CIC variants. *J Inherit Metab Dis* 41:  
1201 169-180, 2018. doi:10.1007/s10545-017-0106-7.
- 1202 131. Porcelli V, Fiermonte G, Longo A, and Palmieri F. The human gene SLC25A29, of solute  
1203 carrier family 25, encodes a mitochondrial transporter of basic amino acids. *J Biol*  
1204 *Chem* 289: 13374-13384, 2014. doi:10.1074/jbc.M114.547448.
- 1205 132. Prasun P, Young S, Salomons G, Werneke A, Jiang YH, Struys E, Paige M, Avantagegiati  
1206 ML, and McDonald M. Expanding the Clinical Spectrum of Mitochondrial Citrate Carrier  
1207 (SLC25A1) Deficiency: Facial Dysmorphism in Siblings with Epileptic Encephalopathy  
1208 and Combined D,L-2-Hydroxyglutaric Aciduria. *JIMD reports* 19: 111-115, 2015.  
1209 doi:10.1007/8904\_2014\_378.
- 1210 133. Prohl C, Pelzer W, Diekert K, Kmita H, Bedekovics T, Kispal G, and Lill R. The yeast  
1211 mitochondrial carrier Leu5p and its human homologue Graves' disease protein are  
1212 required for accumulation of coenzyme A in the matrix. *Mol Cell Biol* 21: 1089-1097,  
1213 2001.
- 1214 134. Rial E, Poustie A, and Nicholls DG. Brown-adipose-tissue mitochondria: the regulation  
1215 of the 32000-Mr uncoupling protein by fatty acids and purine nucleotides. *Eur J*  
1216 *Biochem* 137: 197-203, 1983.
- 1217 135. Robinson AJ, Kunji ER, and Gross A. Mitochondrial carrier homolog 2 (MTCH2): the  
1218 recruitment and evolution of a mitochondrial carrier protein to a critical player in  
1219 apoptosis. *Exp Cell Res* 318: 1316-1323, 2012. doi:10.1016/j.yexcr.2012.01.026.
- 1220 136. Robinson AJ, and Kunji ERS. Mitochondrial carriers in the cytoplasmic state have a  
1221 common substrate binding site. *Proc Natl Acad Sci USA* 103: 2617-2622, 2006.
- 1222 137. Robinson AJ, Overy C, and Kunji ERS. The mechanism of transport by mitochondrial  
1223 carriers based on analysis of symmetry. *Proc Natl Acad Sci USA* 105: 17766-17771,  
1224 2008. doi:Doi 10.1073/Pnas.0809580105.
- 1225 138. Rodriguez-Garcia ME, Cotrina-Vinagre FJ, Cruz-Rojo J, Garzon-Lorenzo L, Carnicero-  
1226 Rodriguez P, Pozo JS, and Martinez-Azorin F. A rare male patient with Fontaine

- 1227 progeroid syndrome caused by p.R217H de novo mutation in SLC25A24. *Am J Med*  
1228 *Genet A* 176: 2479-2486, 2018. doi:10.1002/ajmg.a.40496.
- 1229 139. Rottiers V, Francisco A, Platov M, Zaltsman Y, Ruggiero A, Lee SS, Gross A, and Libert S.  
1230 MTCH2 is a conserved regulator of lipid homeostasis. *Obesity (Silver Spring)* 25: 616-  
1231 625, 2017. doi:10.1002/oby.21751.
- 1232 140. Runswick MJ, Powell SJ, Nyren P, and Walker JE. Sequence of the bovine mitochondrial  
1233 phosphate carrier protein: structural relationship to ADP/ATP translocase and the  
1234 brown fat mitochondria uncoupling protein. *EMBO J* 6: 1367-1373, 1987.
- 1235 141. Ruprecht JJ, Hellowell AM, Harding M, Crichton PG, Mccoy AJ, and Kunji ERS. Structures  
1236 of yeast mitochondrial ADP/ATP carriers support a domain-based alternating-access  
1237 transport mechanism. *Proc Natl Acad Sci USA* 111: E426-E434, 2014. doi:Doi  
1238 10.1073/Pnas.1320692111.
- 1239 142. Ruprecht JJ, King MS, Zogg T, Aleksandrova AA, Pardon E, Crichton PG, Steyaert J, and  
1240 Kunji ERS. The molecular mechanism of transport by the mitochondrial ADP/ATP  
1241 carrier. *Cell* 176: 435-447, 2019. doi:10.1016/j.cell.2018.11.025.
- 1242 143. Ruprecht JJ, and Kunji ERS. The SLC25 Mitochondrial Carrier Family: Structure and  
1243 Mechanism. *Trends Biochem Sci* 2019. doi:10.1016/j.tibs.2019.11.001.
- 1244 144. Ruprecht JJ, and Kunji ERS. Structural changes in the transport cycle of the  
1245 mitochondrial ADP/ATP carrier. *Curr Opin Struct Biol* 57: 135-144, 2019.  
1246 doi:10.1016/j.sbi.2019.03.029.
- 1247 145. Ryu J, Ko JM, and Shin CH. A 9-year-old Korean girl with Fontaine progeroid syndrome:  
1248 a case report with further phenotypical delineation and description of clinical course  
1249 during long-term follow-up. *BMC Med Genet* 20: 188, 2019. doi:10.1186/s12881-019-  
1250 0921-9.
- 1251 146. Saheki T, Inoue K, Tushima A, Mutoh K, and Kobayashi K. Citrin deficiency and current  
1252 treatment concepts. *Mol Genet Metab* 100 Suppl 1: S59-64, 2010.  
1253 doi:10.1016/j.ymgme.2010.02.014.
- 1254 147. Saraste M, and Walker JE. Internal sequence repeats and the path of polypeptide in  
1255 mitochondrial ADP/ATP translocase. *FEBS Lett* 144: 250-254, 1982.
- 1256 148. Schaedler TA, Faust B, Shintre CA, Carpenter EP, Srinivasan V, van Veen HW, and Balk J.  
1257 Structures and functions of mitochondrial ABC transporters. *Biochem Soc Trans* 43:  
1258 943-951, 2015. doi:10.1042/BST20150118.

- 1259 149. Schiff M, Veauville-Merllie A, Su CH, Tzagoloff A, Rak M, Ogier de Baulny H, Boutron A,  
1260 Smedts-Walters H, Romero NB, Rigal O, Rustin P, Vianey-Saban C, and Acquaviva-  
1261 Bourdain C. SLC25A32 Mutations and Riboflavin-Responsive Exercise Intolerance. *N*  
1262 *Engl J Med* 374: 795-797, 2016. doi:10.1056/NEJMc1513610.
- 1263 150. Shamseldin HE, Smith LL, Kentab A, Alkhalidi H, Summers B, Alsedairy H, Xiong Y, Gupta  
1264 VA, and Alkuraya FS. Mutation of the mitochondrial carrier SLC25A42 causes a novel  
1265 form of mitochondrial myopathy in humans. *Hum Genet* 135: 21-30, 2016.  
1266 doi:10.1007/s00439-015-1608-8.
- 1267 151. Shaw GC, Cope JJ, Li L, Corson K, Hersey C, Ackermann GE, Gwynn B, Lambert AJ,  
1268 Wingert RA, Traver D, Trede NS, Barut BA, Zhou Y, Minet E, Donovan A, Brownlie A,  
1269 Balzan R, Weiss MJ, Peters LL, Kaplan J, Zon LI, and Paw BH. Mitoferrin is essential for  
1270 erythroid iron assimilation. *Nature* 440: 96-100, 2006. doi:10.1038/nature04512.
- 1271 152. Smith A, McBride S, Marcadier JL, Michaud J, Al-Dirbashi OY, Schwartzentruber J,  
1272 Beaulieu CL, Katz SL, Consortium FC, Majewski J, Bulman DE, Geraghty MT, Harper ME,  
1273 Chakraborty P, and Lines MA. Severe Neonatal Presentation of Mitochondrial Citrate  
1274 Carrier (SLC25A1) Deficiency. *JIMD reports* 30: 73-79, 2016.  
1275 doi:10.1007/8904\_2016\_536.
- 1276 153. Smith VR, Fearnley IM, and Walker JE. Altered chromatographic behaviour of  
1277 mitochondrial ADP/ATP translocase induced by stabilization of the protein by binding  
1278 of 6'-O-fluorescein-atractyloside. *Biochem J* 376: 757-763, 2003.
- 1279 154. Spaan AN, Ijlst L, van Roermund CW, Wijburg FA, Wanders RJ, and Waterham HR.  
1280 Identification of the human mitochondrial FAD transporter and its potential role in  
1281 multiple acyl-CoA dehydrogenase deficiency. *Mol Genet Metab* 86: 441-447, 2005.
- 1282 155. Spiegel R, Shaag A, Edvardson S, Mandel H, Stepensky P, Shalev SA, Horovitz Y, Pines O,  
1283 and Elpeleg O. SLC25A19 mutation as a cause of neuropathy and bilateral striatal  
1284 necrosis. *Ann Neurol* 66: 419-424, 2009. doi:10.1002/ana.21752.
- 1285 156. Springett R, King MS, Crichton PG, and Kunji ERS. Modelling the free energy profile of  
1286 the mitochondrial ADP/ATP carrier. *Biochim Biophys Acta* 1858: 906-914, 2017.  
1287 doi:10.1016/j.bbabi.2017.05.006.
- 1288 157. Thangaratnarajah C, Ruprecht JJ, and Kunji ERS. Calcium-induced conformational  
1289 changes of the regulatory domain of human mitochondrial aspartate/glutamate  
1290 carriers. *Nat Commun* 5: 5491, 2014. doi:10.1038/ncomms6491.

- 1291 158. Thompson K, Majd H, Dallabona C, Reinson K, King MS, Alston CL, He L, Lodi T, Jones  
1292 SA, Fattal-Valevski A, Fraenkel ND, Saada A, Haham A, Isohanni P, Vara R, Barbosa IA,  
1293 Simpson MA, Deshpande C, Puusepp S, Bonnen PE, Rodenburg RJ, Suomalainen A,  
1294 Ounap K, Elpeleg O, Ferrero I, McFarland R, Kunji ERS, and Taylor RW. Recurrent *de*  
1295 *novo* dominant mutations in SLC25A4 cause severe early-onset mitochondrial disease  
1296 and loss of mitochondrial DNA copy number. *Am J Hum Genet* 99: 860-876, 2016.  
1297 doi:10.1016/j.ajhg.2016.08.014.
- 1298 159. Titus SA, and Moran RG. Retrovirally mediated complementation of the glyB  
1299 phenotype. Cloning of a human gene encoding the carrier for entry of folates into  
1300 mitochondria. *J Biol Chem* 275: 36811-36817, 2000.
- 1301 160. Traba J, Satrustegui J, and Del Arco A. Characterization of SCaMC-3-Like/slc25a41 a  
1302 novel calcium-independent mitochondrial ATP-Mg/Pi carrier. *Biochem J* 2008.
- 1303 161. Visser WF, van Roermund CW, Waterham HR, and Wanders RJ. Identification of human  
1304 PMP34 as a peroxisomal ATP transporter. *Biochem Biophys Res Commun* 299: 494-497,  
1305 2002. doi:S0006291X02026633.
- 1306 162. Vozza A, Blanco E, Palmieri L, and Palmieri F. Identification of the mitochondrial  
1307 GTP/GDP transporter in *Saccharomyces cerevisiae*. *J Biol Chem* 279: 20850-20857,  
1308 2004.
- 1309 163. Vozza A, Parisi G, De Leonardis F, Lasorsa FM, Castegna A, Amorese D, Marmo R,  
1310 Calcagnile VM, Palmieri L, Ricquier D, Paradies E, Scarcia P, Palmieri F, Bouillaud F, and  
1311 Fiermonte G. UCP2 transports C4 metabolites out of mitochondria, regulating glucose  
1312 and glutamine oxidation. *Proc Natl Acad Sci U S A* 111: 960-965, 2014.  
1313 doi:10.1073/pnas.1317400111.
- 1314 164. Wan J, Steffen J, Yourshaw M, Mamsa H, Andersen E, Rudnik-Schoneborn S, Pope K,  
1315 Howell KB, McLean CA, Kornberg AJ, Joseph J, Lockhart PJ, Zerres K, Ryan MM, Nelson  
1316 SF, Koehler CM, and Jen JC. Loss of function of SLC25A46 causes lethal congenital  
1317 pontocerebellar hypoplasia. *Brain* 139: 2877-2890, 2016. doi:10.1093/brain/aww212.
- 1318 165. Wang Y, Langer NB, Shaw GC, Yang G, Li L, Kaplan J, Paw BH, and Bloomer JR.  
1319 Abnormal mitoferrin-1 expression in patients with erythropoietic protoporphyria. *Exp*  
1320 *Hematol* 39: 784-794, 2011. doi:10.1016/j.exphem.2011.05.003.
- 1321 166. Wang Y, and Tajkhorshid E. Electrostatic funneling of substrate in mitochondrial inner  
1322 membrane carriers. *Proc Natl Acad Sci USA* 105: 9598-9603, 2008.

- 1323 167. Wibom R, Lasorsa FM, Tohonen V, Barbaro M, Sterky FH, Kucinski T, Naess K, Jonsson  
1324 M, Pierri CL, Palmieri F, and Wedell A. AGC1 deficiency associated with global cerebral  
1325 hypomyelination. *N Engl J Med* 361: 489-495, 2009. doi:10.1056/NEJMoa0900591.
- 1326 168. Writzl K, Maver A, Kovacic L, Martinez-Valero P, Contreras L, Satrustegui J, Castori M,  
1327 Faivre L, Lapunzina P, van Kuilenburg ABP, Radovic S, Thauvin-Robinet C, Peterlin B, Del  
1328 Arco A, and Hennekam RC. De Novo Mutations in SLC25A24 Cause a Disorder  
1329 Characterized by Early Aging, Bone Dysplasia, Characteristic Face, and Early Demise.  
1330 *Am J Hum Genet* 101: 844-855, 2017. doi:10.1016/j.ajhg.2017.09.017.
- 1331 169. Yang Q, Bruschiweiler S, and Chou JJ. A self-sequestered calmodulin-like Ca<sup>2</sup>(+) sensor  
1332 of mitochondrial S<sub>Ca</sub>MC carrier and its implication to Ca<sup>2</sup>(+)-dependent ATP-Mg/P(i)  
1333 transport. *Structure* 22: 209-217, 2014. doi:10.1016/j.str.2013.10.018.
- 1334 170. Ye X, Xu J, Cheng C, Yin G, Zeng L, Ji C, Gu S, Xie Y, and Mao Y. Isolation and  
1335 characterization of a novel human putative anemia-related gene homologous to  
1336 mouse sideroflexin. *Biochem Genet* 41: 119-125, 2003. doi:10.1023/a:1022026001114.
- 1337 171. Yoneshiro T, Wang Q, Tajima K, Matsushita M, Maki H, Igarashi K, Dai Z, White PJ,  
1338 McGarrah RW, Ilkayeva OR, Deleye Y, Oguri Y, Kuroda M, Ikeda K, Li H, Ueno A, Ohishi  
1339 M, Ishikawa T, Kim K, Chen Y, Sponton CH, Pradhan RN, Majd H, Greiner VJ, Yoneshiro  
1340 M, Brown Z, Chondronikola M, Takahashi H, Goto T, Kawada T, Sidossis L, Szoka FC,  
1341 McManus MT, Saito M, Soga T, and Kajimura S. BCAA catabolism in brown fat controls  
1342 energy homeostasis through SLC25A44. *Nature* 572: 614-619, 2019.  
1343 doi:10.1038/s41586-019-1503-x.
- 1344 172. Zaltsman Y, Shachnai L, Yivgi-Ohana N, Schwarz M, Maryanovich M, Houtkooper RH,  
1345 Vaz FM, De Leonardis F, Fiermonte G, Palmieri F, Gillissen B, Daniel PT, Jimenez E,  
1346 Walsh S, Koehler CM, Roy SS, Walter L, Hajnoczky G, and Gross A. MTCH2/MIMP is a  
1347 major facilitator of tBID recruitment to mitochondria. *Nat Cell Biol* 12: 553-562, 2010.  
1348 doi:10.1038/ncb2057.
- 1349 173. Zarrilli R, Oates EL, McBride OW, Lerman MI, Chan JY, Santisteban P, Ursini MV,  
1350 Notkins AL, and Kohn LD. Sequence and chromosomal assignment of a novel cDNA  
1351 identified by immunoscreening of a thyroid expression library: similarity to a family of  
1352 mitochondrial solute carrier proteins. *Mol Endocrinol* 3: 1498-1505, 1989.  
1353 doi:10.1210/mend-3-9-1498.
- 1354





1356 **Legends to the figures**

1357

1358 **FIGURE 1. The role of the human mitochondrial carrier family (SLC25) in metabolism and**  
1359 **mitochondrial function**

1360 Schematic representation of the mammalian mitochondrion. Shown in green are the  
1361 electron transfer chain complexes, bottom to top; glycerophosphate dehydrogenase, fatty  
1362 acid-dehydrogenase-electron transfer flavoprotein, dihydroorotate dehydrogenase, and  
1363 complex I to IV with cytochrome c. Shown in blue is the dimer of ATP synthase and in  
1364 red/orange the mitochondrial pyruvate carrier heterodimer (MPC). Shown in purple and  
1365 yellow are unidentified and identified mitochondrial carriers, respectively: AAC1-4, ADP/ATP  
1366 carriers; AGC1-2, aspartate/glutamate carriers; APC1-4, ATP-Mg/Pi carriers; BAC, basic  
1367 amino acid carrier; CAC, carnitine-acylcarnitine carrier; CIC, citrate carrier; DIC, dicarboxylate  
1368 carrier; GC1-2, glutamate carriers; GLYC, glycine carrier; MTFRN1-2 mitoferrins; ODC,  
1369 oxoadipate carrier; OGC, oxoglutarate carrier; ORC1-2, ornithine carriers; PIC, phosphate  
1370 carrier; SAMC, S-adenosylmethionine carrier; TPC, thiamine pyrophosphate carrier; UCP1,  
1371 uncoupling protein; UCP2, uncoupling-like protein 2. CS, cytosol; IS, intermembrane space;  
1372 OM outer membrane; IM inner membrane; MM mitochondrial matrix.

1373

1374

1375 **FIGURE 2. Structures of the mitochondrial ADP/ATP carrier and the calcium-regulated ATP-**  
1376 **Mg/phosphate carrier and aspartate/glutamate carrier**

1377 Structures of three different mitochondrial carriers, based on PDB entries 1OKC (128) and  
1378 4C9Q (141) for the carrier domains and 4P5W (157) and 4ZCU (59) for the calcium-regulatory  
1379 domains. (A) The mitochondrial ADP/ATP carrier. (B) The mitochondrial ATP-Mg/Pi carrier  
1380 consists of three domains; (i) N-terminal calcium-regulatory domain with four EF-hands (EF1-  
1381 4), each binding calcium, (ii) amphipathic helix and (iii) C-terminal carrier domain. (C) The  
1382 aspartate/glutamate carrier also has a three-domain structure, but with a different order; (i)  
1383 N-terminal calcium-regulatory domain, (ii) carrier domain, and (iii) C-terminal amphipathic  
1384 helix. The N-terminal domain has eight EF-hand folds, but only EF-hand 2 is capable of  
1385 binding calcium, which together with EF-hands 1 and 3 forms a calcium-responsive mobile  
1386 unit. EF-hands 4–8 have evolved to form a static dimerization interface. The structures are  
1387 shown in a cartoon representation, colored from the N-terminus in blue to the C-terminus in

1388 red. Also shown are the canonical substrates as well as calcium ions (green), magnesium ion  
1389 (chartreuse) and protons (white) in sphere representations. IS, intermembrane space; OM  
1390 outer membrane; IM inner membrane; MM mitochondrial matrix.

1391

1392

1393 **FIGURE 3. Mitochondrial carriers have a three-fold pseudo-symmetrical structure**

1394 (A) Aligned amino acid sequences of the three repeats of the human ADP/ATP carrier AAC1  
1395 (ANT1). Symmetrically conserved residues are shown in the consensus sequence and as bars,  
1396 when present in at least two out of three repeats. (B) and (C). Comparative model of the  
1397 human ADP/ATP carrier, based on PDB:1OKC (128), viewed from the membrane and the  
1398 intermembrane space, respectively. Shown also is the three-fold pseudo-symmetrical axis,  
1399 symbolized by an equilateral triangle. Odd-numbered (H1, H3, H5), matrix (h12, h34, h56),  
1400 linker (l12, l34, l56) and even-numbered helices (H2, H4, H6) are shown in primary colors for  
1401 the core elements and in gray for the gate elements (142). The black spheres with roman  
1402 numerals show the positions of the three contact points of the substrate binding site (94,  
1403 136). The example, triplet 8-113-210, is indicated by a rectangle across the three repeats in  
1404 (A) and by cyan spheres in (B). IS, intermembrane space; IM inner membrane; MM  
1405 mitochondrial matrix.

1406

1407

1408 **FIGURE 4. Alternating access transport mechanism for the mitochondrial ADP/ATP carrier.**

1409 Lateral view from the membrane of the mitochondrial ADP/ATP carrier in the cytoplasmic  
1410 state (left) and matrix state (right). Shown are the cytoplasmic state of the bovine ADP/ATP  
1411 carrier (PDB:1OKC) (128) and the matrix state of the ADP/ATP carrier of *Thermothelomyces*  
1412 *thermophila* (PDB:6GCI) (142). The water-accessible surfaces are shown in light blue. Also  
1413 indicated are the three main functional features; cytoplasmic gate, substrate binding site  
1414 and matrix gate. The black spheres with roman numerals are the contact points of the  
1415 substrate binding site (94, 136). Shown in green are residues that most likely bind the  
1416 adenine nucleotide substrates. IS, intermembrane space; IM inner membrane; MM  
1417 mitochondrial matrix.

1418

1419

1420 **FIGURE 5. Structural changes in the transport cycle of the human mitochondrial ADP/ATP**  
1421 **carrier**

1422 (A) View from the intermembrane space and (B) lateral view from the membrane of the  
1423 human ADP/ATP carrier in the cytoplasmic state (left) and matrix state (right). For the import  
1424 of ADP, conformational changes involve the simultaneous outward rotation of the core  
1425 elements, shown in primary colors, and inward rotation of the gate elements, shown in gray,  
1426 in a coordinated way (142). For the export of ATP, the converse happens. Substrate binding  
1427 increases the probability of the state interconversion (156). The structural models are based  
1428 on the structures of the cytoplasmic state of the bovine ADP/ATP carrier (PDB:1OKC) (128)  
1429 and the matrix state of the ADP/ATP carrier of *Thermothelomyces thermophila* (PDB:6GCI)  
1430 (142). The black spheres with roman numerals are the contact points of the substrate  
1431 binding site (94, 136). IS, intermembrane space; IM inner membrane; MM mitochondrial  
1432 matrix.

1433

1434

1435 **FIGURE 6. Pathogenic mutations observed in disease variants of mitochondrial carriers**

1436 Aligned triplets of the 16 mitochondrial carriers associated with developmental, metabolic  
1437 and neuromuscular diseases. The mutations that have a severe effect on function are shown  
1438 in red boxes, whereas those that have milder effects are in yellow. Mutations in blue boxes  
1439 have been identified by genetic analysis, but their effect has not been studied  
1440 experimentally. At the bottom are the three residue numbers that form a triplet in the  
1441 human ADP/ATP carrier (SLC25A4). At the top are the conserved structural and functional  
1442 features of mitochondrial carriers. The triplet is labelled by the one-letter code of the most  
1443 conserved residue or by the most common property:  $\pi$  small amino acids,  $\Phi$  hydrophobic  
1444 amino acids,  $\xi$  hydrophilic amino acids,  $\Omega$  aromatic amino acids, or by X for any amino acid.  
1445 The black spheres with roman numerals are the contact points of the substrate binding site  
1446 (94, 136). H6 in the ADP/ATP carrier is one residue shorter than other carriers and lacks a  
1447 residue in triplet 90. The matrix loops (indicted by the black bar), as well as the cytoplasmic  
1448 loops and N- and C-terminus have been omitted.

1449

1450

1451 **FIGURE 7. Small amino acid residues on the odd-numbered helices**

1452 (A) View from the intermembrane space and (B) lateral view from the membrane of the  
1453 human ADP/ATP carrier in the cytoplasmic state (left) and matrix state (right). The structural  
1454 models are based on the structures of the cytoplasmic state of the bovine ADP/ATP carrier  
1455 (128) and the matrix state of the ADP/ATP carrier of *Thermothelomyces thermophila* (142).  
1456 The carrier is shown in surface representation and the helices in cartoon representation with  
1457 the core elements in primary colors and the gate elements in gray. Glycine or small residues  
1458 in the interface with the preceding helix are shown in pink, whereas those in the interface  
1459 with the following helix are shown in magenta. The sequence motif is  $\pi G\pi\chi\pi G\chi\chi\pi\chi\chi\pi$   
1460 where G stands for glycine and  $\pi$  for small amino acids (142-144). When the carrier changes  
1461 from the cytoplasmic state to the matrix state the inter-helical distances become smaller on  
1462 the cytoplasmic side of the carrier to facilitate the formation of the cytoplasmic network,  
1463 requiring small residues in the helical interfaces. IS, intermembrane space; IM inner  
1464 membrane; MM mitochondrial matrix.

1465

1466

1467 **FIGURE 8. Key amino acid residues of the matrix gate**

1468 (A) View from the intermembrane space and (B) lateral view from the membrane of the  
1469 human ADP/ATP carrier in the cytoplasmic state (left) and matrix state (right). The structures  
1470 are described in the legend to FIGURE 7. The key residues shown belong to the sequence  
1471 motif  $Px[DE]xx[RK]xxxQ$  on the odd-numbered helices. The proline residues (orange) are  
1472 found at the pronounced kink in the odd-numbered helices, bringing the negatively charged  
1473 (red) and positively charged (blue) residues together to form the matrix network in the  
1474 cytoplasmic state. Underneath one of the salt bridges is a glutamine residue (green) that  
1475 forms hydrogen bonds with both residues (glutamine brace), but in other carriers one, two  
1476 or three glutamine braces can be found (FIGURE 6) (141). IS, intermembrane space; IM inner  
1477 membrane; MM mitochondrial matrix.

1478

1479

1480 **FIGURE 9. Detailed view of one of the three binding sites for cardiolipin**

1481 One cardiolipin molecule is shown in ball-and-stick representation (cdl802, PDB: 2C3E),  
1482 which is bound on the surface of the carrier and spans the inter-domain interface. The  
1483 carrier is shown in cartoon representation with transmembrane H4 (yellow and gray) and

1484 matrix helix h56 (red) enhanced. The two phosphate groups of cardiolipin, which are linked  
1485 by a glycerol moiety, form hydrogen bonds with the amide groups (128) and interact with  
1486 the positively-charged ends of the helix dipoles of the N-terminal ends of the matrix helices  
1487 (cardiolipin binding site I) and the even-numbered helices (cardiolipin binding site II) (24,  
1488 141, 142). The four fatty acid chains of cardiolipin interact with the surface of the carrier in a  
1489 non-specific way via van der Waals interactions (41). Residues in the conserved cardiolipin  
1490 binding site I and II are shown as green and purple sticks, respectively. The interface  
1491 between domain 2 and 3 is shown as a dashed line.

1492

1493

1494 **FIGURE 10. Amino acid residues involved in cardiolipin binding**

1495 (A) View from the intermembrane space and (B) lateral view from the membrane of the  
1496 human ADP/ATP carrier in the cytoplasmic state (left) and matrix state (right). The structures  
1497 are described in the legend to FIGURE 7. There are three highly conserved binding sites for  
1498 cardiolipin in the mitochondrial ADP/ATP carrier. The residues of cardiolipin binding site I  
1499 belong to the [YF]xG motif (green), whereas those of cardiolipin binding site II belong to the  
1500 [YWF][RK]G motif (purple) (128, 141, 142). IS, intermembrane space; IM inner membrane;  
1501 MM mitochondrial matrix.

1502

1503

1504 **FIGURE 11. Amino acid residues important for the domain structures on the matrix side**

1505 (A) View from the intermembrane space and (B) lateral view from the membrane of the  
1506 human ADP/ATP carrier in the cytoplasmic state (left) and matrix state (right). The structures  
1507 are described in the legend to FIGURE 7. The positively charged residue of the E-R link I  
1508 (blue), which is located in the matrix gate area, interacts with the negatively charged residue  
1509 of the E-R link II, which is located on the matrix helices. The N-terminal and the fourth  
1510 residues of the linker helices are most commonly glycine residues (magenta), although the  
1511 latter can be replaced by other small residues. IS, intermembrane space; IM inner  
1512 membrane; MM mitochondrial matrix.

1513

1514

1515 **FIGURE 12. Amino acid residues of the substrate binding site**

1516 (A) View from the intermembrane space and (B) lateral view from the membrane of the  
1517 human ADP/ATP carrier in the cytoplasmic state (left) and matrix state (right). The structures  
1518 are described in the legend to FIGURE 7. The black spheres with roman numerals are the  
1519 contact points of the substrate binding site, which are involved in binding of the substrates  
1520 (94, 136). Other residues in this site (green) may either bind substrate directly, or may allow  
1521 the binding. IS, intermembrane space; IM inner membrane; MM mitochondrial matrix.

1522

1523

1524 **FIGURE 13. Small amino acid residues on the even-numbered helices**

1525 (A) View from the intermembrane space and (B) lateral view from the membrane of the  
1526 human ADP/ATP carrier in the cytoplasmic state (left) and matrix state (right). The structures  
1527 are described in the legend to FIGURE 7. The small residues (chartreuse) in the interhelical  
1528 interfaces with the odd-number helices facilitate conformational changes. Some residues are  
1529 larger, such as the phenylalanine on H6, because their side chains face the membrane in  
1530 both conformations. IS, intermembrane space; IM inner membrane; MM mitochondrial  
1531 matrix.

1532

1533

1534 **FIGURE 14. Amino acid residues of the cytoplasmic gate**

1535 (A) View from the intermembrane space and (B) lateral view from the membrane of the  
1536 human ADP/ATP carrier in the cytoplasmic state (left) and matrix state (right). The structures  
1537 are described in the legend to FIGURE 7. The key residues belong to the sequence motif  
1538  $\xi$ [FY]xx[YF][DE]xx[RK]. The negatively charged (red) and positively charged (blue) residues  
1539 together form the cytoplasmic network in the matrix state. Underneath are aromatic  
1540 residues (orange), which are part of the hydrophobic plug that closes the cytoplasmic gate.  
1541 The aromatic residue preceding the negatively charged residue is the tyrosine brace (Y-  
1542 brace) (142-144). Preceding the aromatic residues are hydrophilic residues ( $\xi$ ), which form  
1543 the ceiling of the substrate binding site. IS, intermembrane space; IM inner membrane; MM  
1544 mitochondrial matrix.

1545

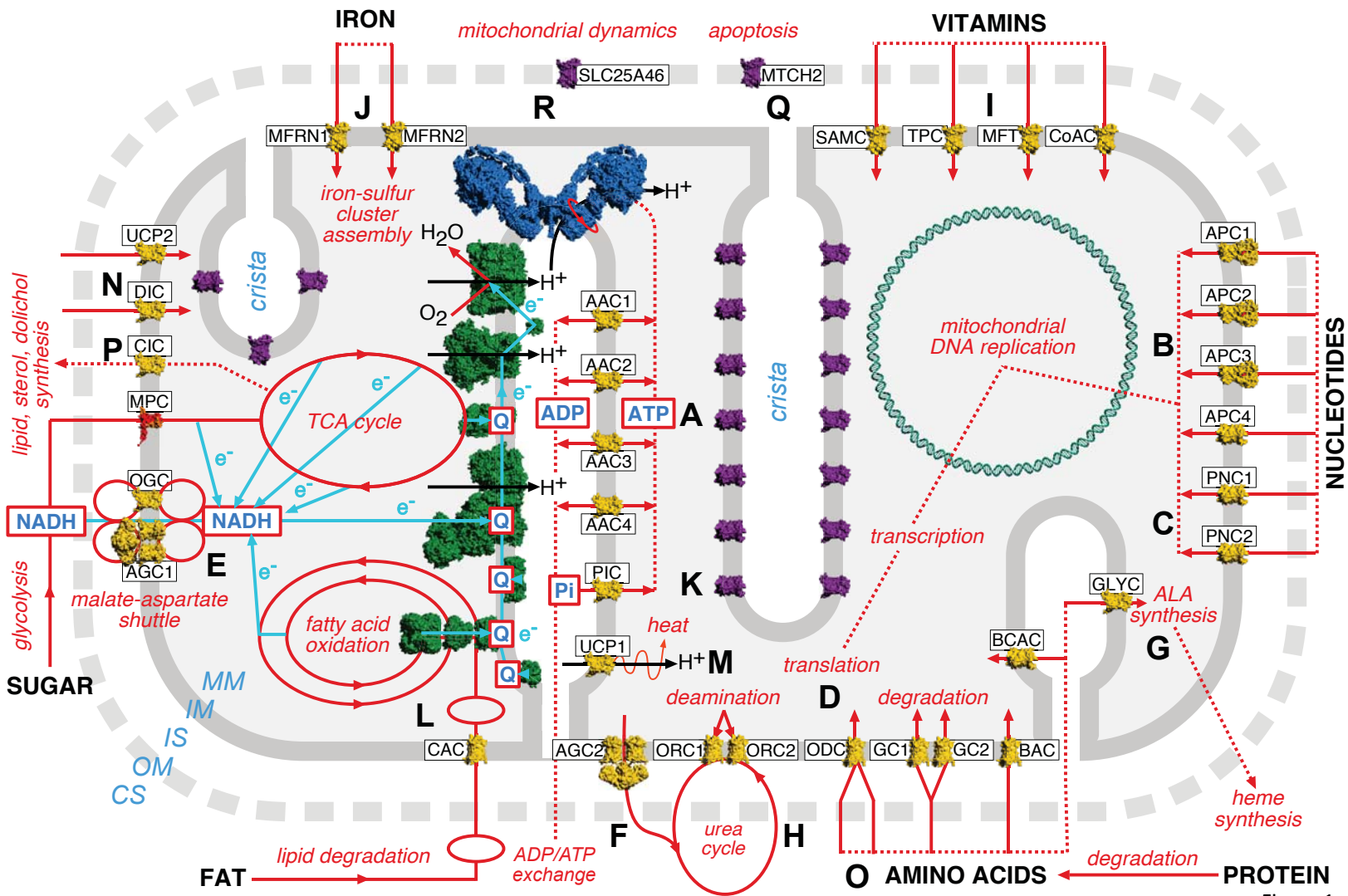
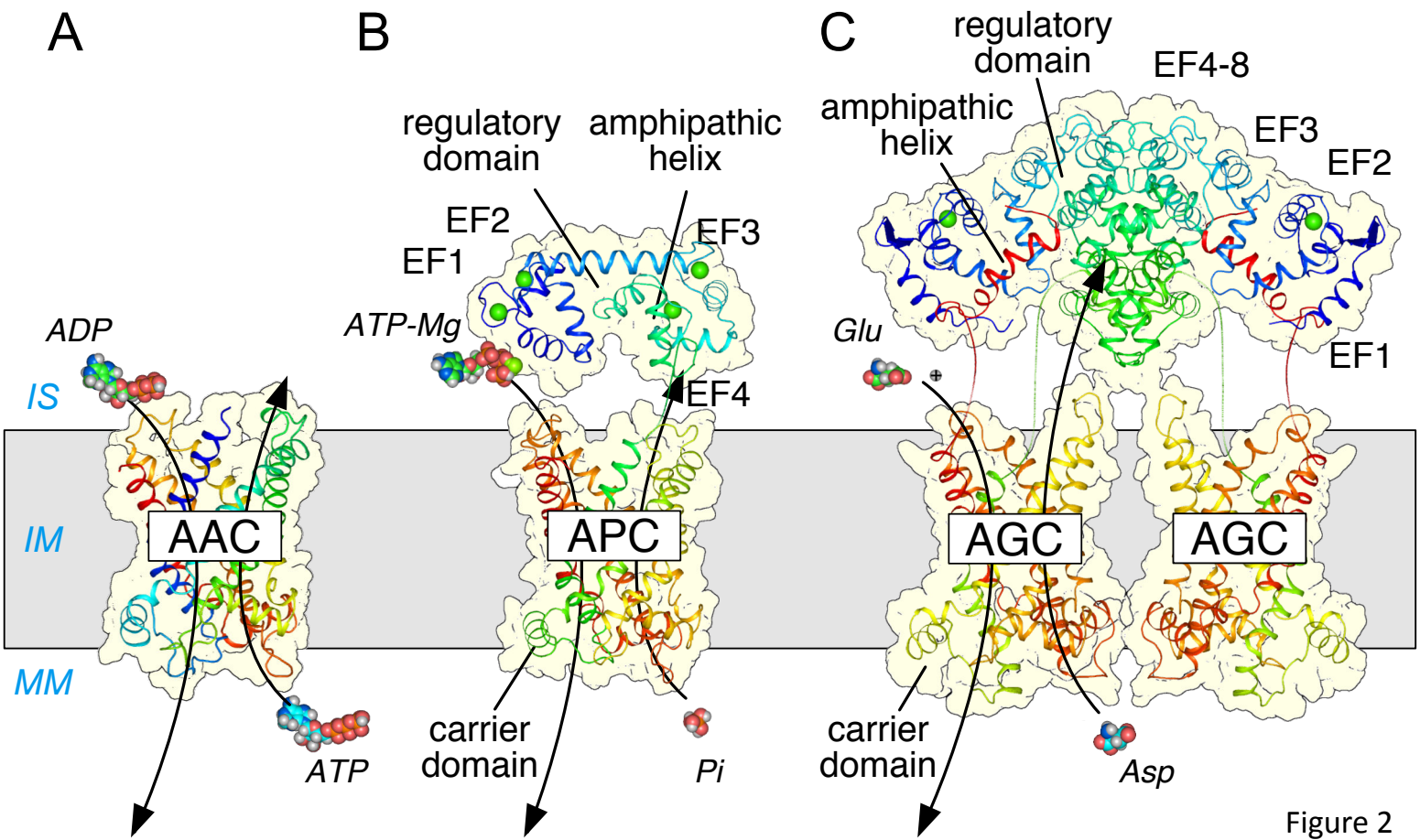


Figure 1





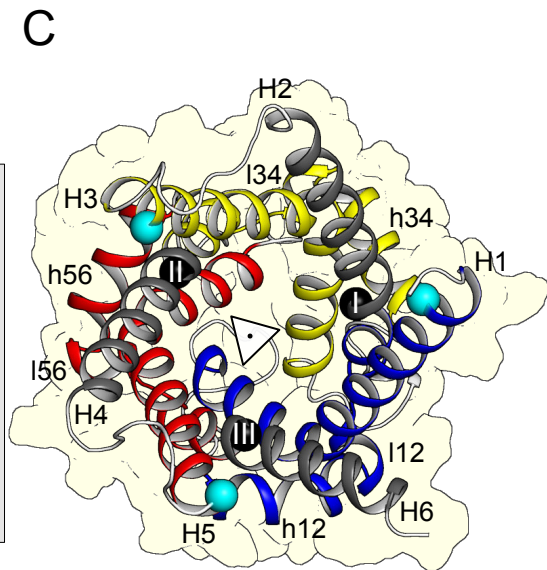
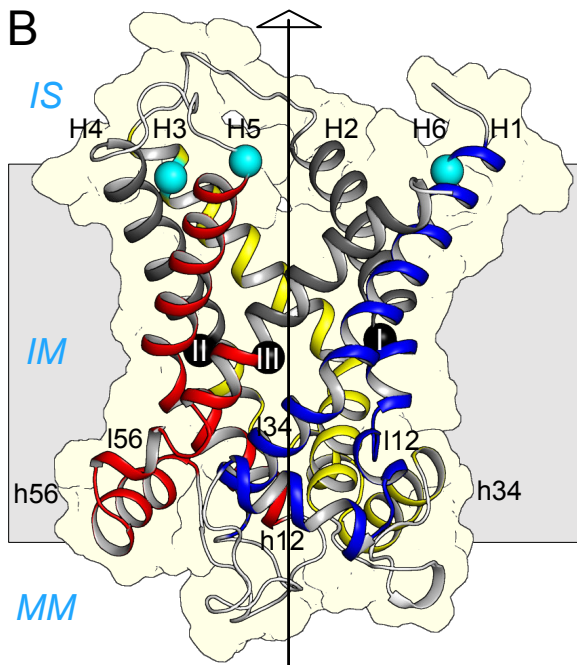
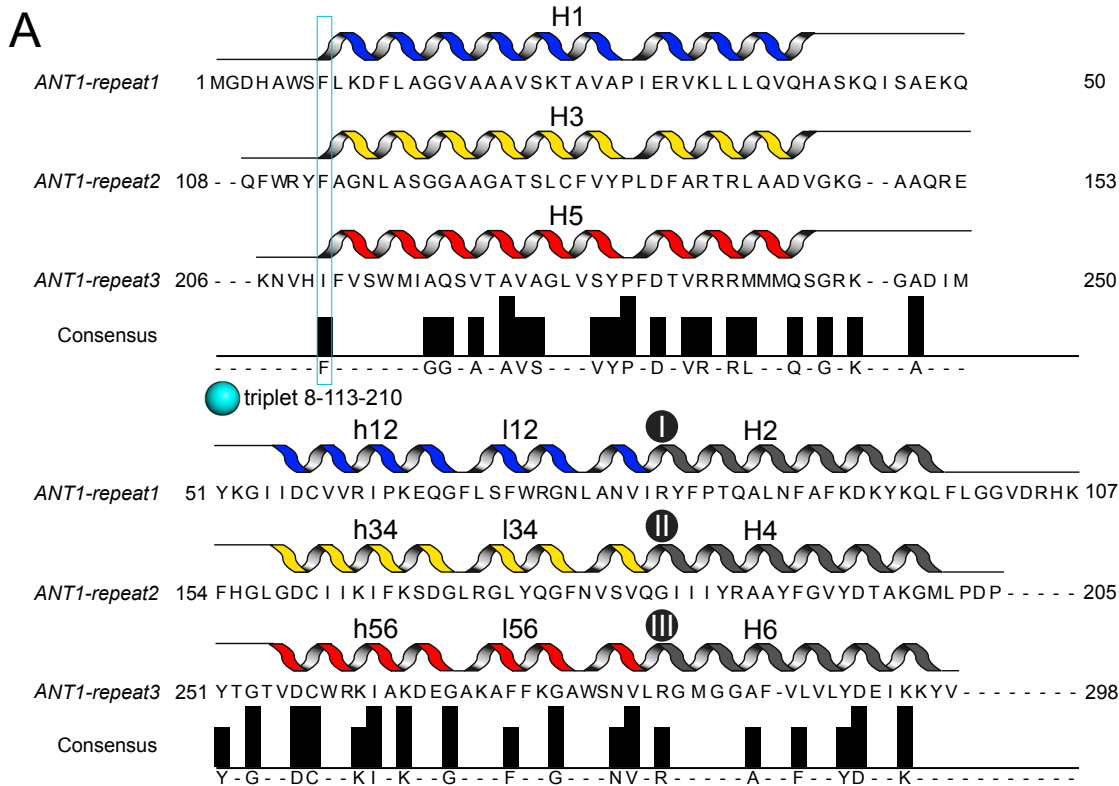
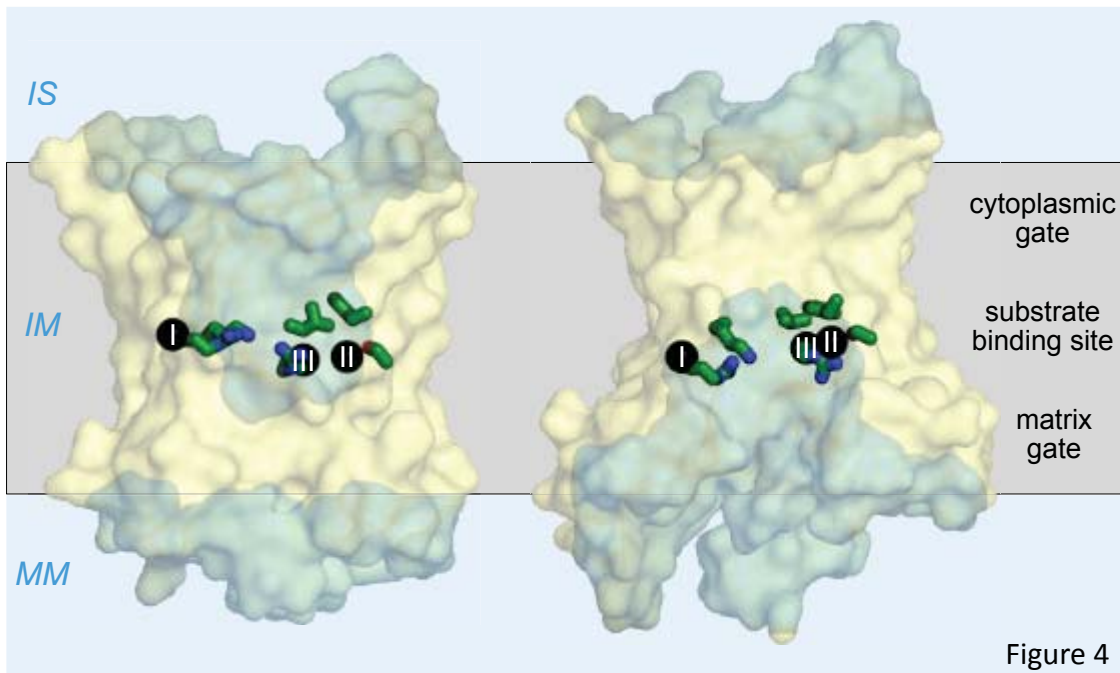


Figure 3

*cytoplasmic state*

*matrix state*



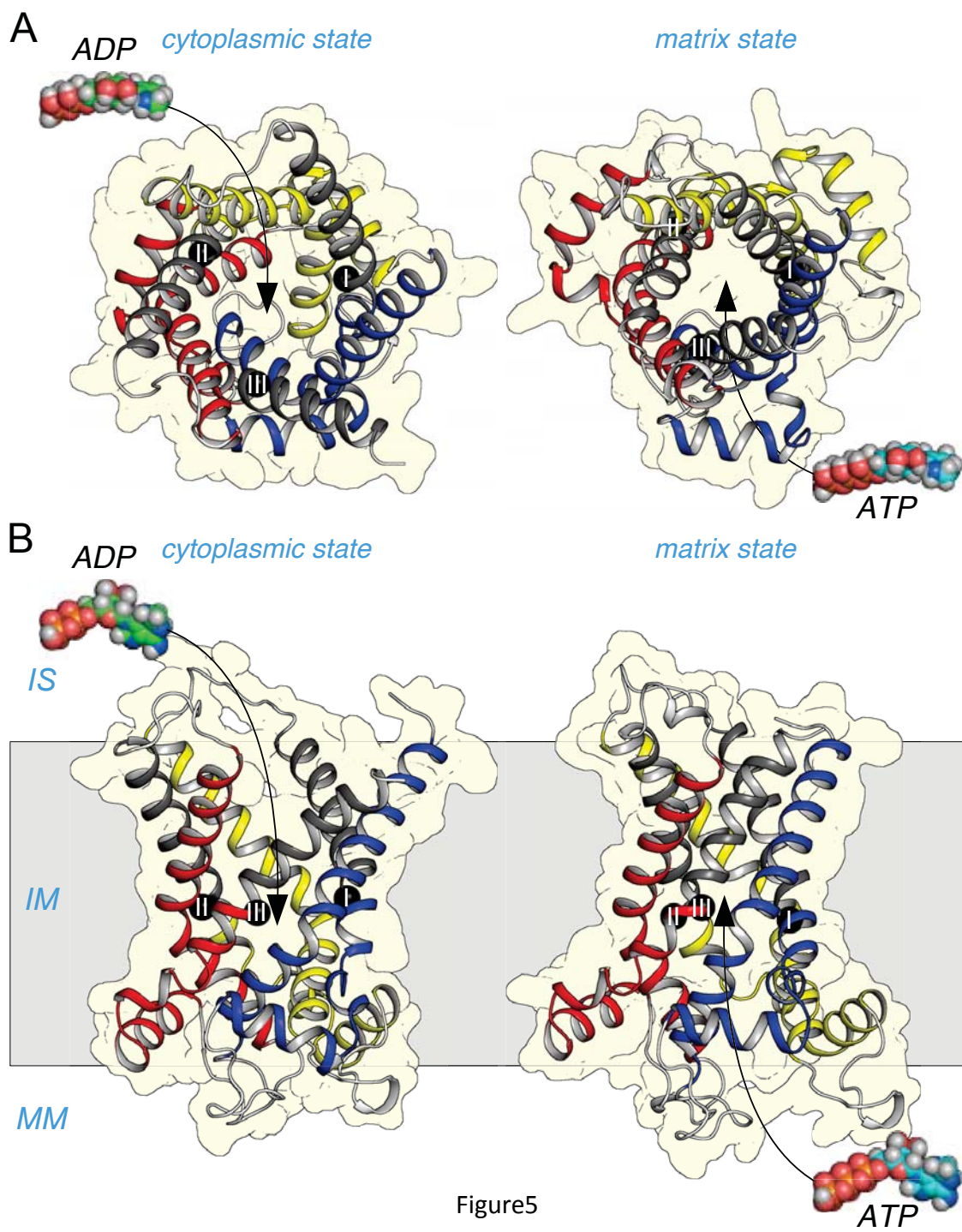


Figure5

small amino acids

	Φ	Φ	Φ	ξ	Φ	Φ	Π	G	Π	Φ	Π	G	Φ	Φ	Π	ξ	Φ	Φ	Π	ξ
SLC25A01	PTP	GRL	KGI	ALT	ILG	LCV	AGF	GLG	GCA	LAI	AGA	GVG	GAA	IEA	EAS	IVV	CVF	IVG	TVN	FCT
SLC25A03	FTL	ISV	LLV	CYT	GLF	LAV	GAA	GGG	IAY	ISI	SAA	CEG	GFV	TFF	TAC	HDA	TII	AAV	LLS	VAH
SLC25A04	FFI	LAF	KGV	DNS	FLW	LAM	ASI	GGA	GGQ	VAS	AV	AGT	AAA	VTV	SSA	KLK	TCL	AFV	VVS	AYY
SLC25A12	SLG	APL	YAN	REL	FVL	TLA	LAA	GGG	SGA	VCM	AAA	GGG	AGV	VSP	GQA	AVA	TIS	AFL	VTV	YNT
SLC25A13	SLP	AAG	YAS	REL	FIL	GLL	LAA	GGG	SGA	VCI	AAA	GGG	AGM	VSP	GQA	AVA	TIS	AFL	VTV	YNT
SLC25A15	ADP	ALV	IQP	DNL	LAM	TAL	AAS	GGG	ASG	AFV	GAG	GGG	TAI	AFC	CAL	VAV	LLL	TVA	GLV	QCY
SLC25A16	WHT	LVH	RHV	SRN	FLL	LML	AAC	GGG	GGG	IMV	AAA	GGG	CMA	CTI	AAA	KVQ	TIT	TCI	VTS	AYY
SLC25A19	KFN	FSL	QVQ	VHN	AFL	VVL	ACC	GGG	SGS	VLG	SAA	GAG	LCV	VMI	TAS	RTK	ALT	LTL	IVT	SHY
SLC25A20	PYA	LPP	KQR	NLI	LFL	LAV	AAA	GGG	GMG	FLI	GSA	GGG	VVI	FFF	LTN	VTW	FGA	VIV	GMA	HTI
SLC25A21	AAF	SLW	RTR	QFK	IAF	VIG	AAI	GGG	GLL	SGL	ASS	GGG	LLT	VTI	EEA	IAS	CIV	LVI	MVN	HNI
SLC25A22	LLF	PLY	AKV	KES	LMF	ILL	NAA	GGG	GCC	IGV	AAA	GGG	LTS	ICA	GQA	VVA	TIV	CVA	VTV	FTN
SLC25A24	WTV	WFM	REV	QRL	LFL	LIG	ASC	GGG	GSA	IML	AAA	GGG	AAT	VTC	SAG	RQQ	TTL	SFA	TIS	AYY
SLC25A26	FPS	VMW	AKQ	AHS	LMA	VLV	AAC	GAG	GSA	VAF	AGA	GEG	VVG	SVF	VAA	DCA	LLA	IVV	LRT	FVT
SLC25A38	VAP	ILI	KET	ASN	FVF	LMS	CLC	GGG	SVI	IGF	SSA	GRC	TSI	CVL	SAA	TGS	LVL	LCV	FMT	QSQ
SLC25A42	VPP	LWF	SPE	SRR	LLM	LFI	SAF	GGG	AAA	LFC	AAA	GGG	ATL	LTI	AAG	KAQ	TSS	ALA	VTS	AYY
SLC25A46	RSY	FPF	AKP	GQE	FIL	GGI	IEA	GHN	LLF	ALA	SLA	LKS	FSL	TLC	ETS	NYD	VVV	LVI	AAL	HMY
Repeat 1	8	9	10	11	12	13	14	15	16	17	18	19	20	21	22	23	24	25	26	27
Repeat 2	113	114	115	116	117	118	119	120	121	122	123	124	125	126	127	128	129	130	131	132
Repeat 3	210	211	212	213	214	215	216	217	218	219	220	221	222	223	224	225	226	227	228	229

matrix gate

	proline kink	matrix network	E-R link I	glutamine brace	cardiolipin binding site I															
	P	D/E	X	Φ	K/R	ξ	R	Φ	Q	ξ	ξ	Y	R/K	G	Φ	Φ	ξ	Π	Φ	
SLC25A01	PPP	TML	EDD	YTV	VII	KKK	TVT	QKR	LFM	QIQ	LHG	DDL	YYY	RRR	GGN	IFT	GFW	DHD	CQC	VVG
SLC25A03	PPP	LMA	DED	LAS	VAV	KKV	CVS	RVR	MIL	QQN	VTK	DQE	YA-	KN-	GT-	FR-	ND-	GA-	FAA	
SLC25A04	PPP	ILF	EDD	RFT	VAV	KRR	LTR	LRR	LIM	QAM	VAM	QDQ	YFY	KHT	GGG	ILT	IGV	DDD	CCC	VIW
SLC25A12	PPP	ILA	DED	LIV	VVI	KKK	TIT	RRR	MIL	QQQ	NVV	QAA	YTY	KTS	NGG	SPV	FRI	DVD	CSC	FAF
SLC25A13	PPP	LLA	DED	LIV	VVI	KKK	TIT	RRR	MIL	QQQ	NVV	QAA	YTY	KTS	NGG	SPV	FRI	DVD	CSC	FAF
SLC25A15	PPP	FTV	DDD	TLC	MVI	KKK	VCS	KRR	MLI	QQQ	TTV	FML	YQQ	RNA	GTG	LVF	TWI	DSR	CVT	CIF
SLC25A16	PPP	LLF	DDD	RMV	VVT	KRR	VVR	LRR	LLM	QAQ	AFI	HQG	HTL	LGT	GGM	VIR	FID	SHT	AAM	LFK
SLC25A19	PPP	FVL	DDD	VVL	ILF	KRK	ITK	RRR	FFL	QAQ	LAV	QQG	YYY	HNK	GTG	ILL	LRM	QHD	AAC	SVA
SLC25A20	PPP	LGP	DED	TRV	VIL	KKK	VCS	RLR	LLF	QQQ	TIT	QQA	YYP	STN	GGG	TF	FLR	DDD	CCV	FAL
SLC25A21	PPP	LFV	DED	VVV	VVA	KKK	TVS	RGR	FLI	QQQ	IAG	QNP	YSY	KTR	SST	LTC	VVF	DDG	SYT	FAM
SLC25A22	PPP	IMC	DED	LMV	ALV	KKK	TIT	RQR	LLL	QQQ	NDS	QAL	YRY	TPS	STG	MAI	STL	DQD	CLC	LTA
SLC25A24	PPP	LML	DEA	FVL	LMV	KKR	ITT	MRR	MLM	QAQ	VVA	HQG	KYQ	MSL	NGN	IIM	FYV	GDG	GCL	FAF
SLC25A26	PPP	LSL	DED	TVV	IVA	KKK	TQT	RRR	LAI	QQT	SVL	PSA	-SD	-TG	-RN	-TV	-FL	-QS	-IV	-FL
SLC25A38	PPP	LIA	DTD	LVV	LTI	KKK	TTT	RRH	LYM	QEQ	TSL	LGY	RYF	VEQ	GSW	MII	LYG	AAQ	VAA	LLV
SLC25A42	PPP	LIA	DDD	RLV	TVV	KRR	IAR	IRR	FMM	QAQ	VVT	STA	AYA	KSS	ENI	AIA	FFR	RHT	VVL	LFR
SLC25A46	PPP	CFL	IYE	VST	LAV	RSL	RLH	QIR	CEL	QTH	VVI	NQQ	P-Y	F-E	T-G	V-M	I-R	N-D	I-C	MGI
Repeat 1	28	29	30	31	32	33	34	35	36	37	38	39	51	52	53	54	55	56	57	58
Repeat 2	133	134	135	136	137	138	139	140	141	142	143	144	154	155	156	157	158	159	160	161
Repeat 3	230	231	232	233	234	235	236	237	238	239	240	241	251	252	253	254	255	256	257	258

E-R link II

cardiolipin binding site II

	ξ	ξ	Φ	Φ	ξ	ξ	E	G	Φ	Φ	G	Φ	Ω	R/K	G	Φ	Φ	Π	ξ	Φ
SLC25A01	RRL	QEQ	TII	VVL	RRK	SEK	HQE	GGG	VLL	LKK	GGA	LTF	YYY	RQK	GGG	LLT	STV	SAP	LTR	LVL
SLC25A03	SPS	VKL	TMV	LYL	KKK	EER	DEL	GGG	VLF	RKK	GAG	LTV	AYW	KKK	GGG	WVL	AAF	PPA	TLR	FWI
SLC25A04	VIR	RKK	III	PFA	KKK	ESD	QDE	GGG	FLA	LRK	SGA	FLF	WYF	RQK	GGG	NFA	LNW	AVS	NSN	VVV
SLC25A12	KLR	RKK	VVI	LLL	RRR	YDE	ELE	GGG	FIP	FFS	GGA	LLF	YYW	RKK	GGG	LAT	IKA	PAA	QCR	LFV
SLC25A13	KLR	KSK	VVI	LVL	RRR	YDE	ELE	GGG	FFP	FFK	GGA	LIL	YYW	RKK	GGG	LAA	LKG	PAA	QCR	LFV
SLC25A15	LKI	KSN	TIV	YLV	SRK	QKN	VDE	GGG	FPI	RLT	GGG	FFL	YYY	KHS	GGG	TLL	SSK	PSP	ATT	LLM
SLC25A16	RKY	ATV	VIV	PYG	QAH	KKH	EEG	GGI	FFR	LFK	GGG	LLF	YYY	KRR	GGG	NLL	GMS	APL	MTN	MIV
SLC25A19	RGK	QTK	IMV	LYL	QRQ	ESK	EEE	GGG	PPA	TQL	AVG	FFF	WYF	KKK	GGG	HLL	VAS	PPP	ATS	QLL
SLC25A20	RKR	KKE	TLL	LYI	FQR	RED	EFE	GGG	IIV	TRT	GGG	LIL	YYY	RKK	GGG	MTF	AVN	ALA	PTV	ILM
SLC25A21	RRA	MQT	IIV	FIY	QKQ	MKE	EEE	GGG	LLI	FQL	GGA	FLL	YNY	KKK	GGG	ILL	LTL	PAP	PTK	ILI
SLC25A22	IRR	KDK	TLI	VLL	RRR	SSH	ERE	GGG	YIP	FAS	GGA	MLF	YYL	RKK	GGG	ALA	AGY	VAC	NTR	LLA
SLC25A24	RKR	QKR	MII	VLI	KKS	EHK	GEE	GGG	ILI	RGP	SAG	LFL	WYY	RKR	GGG	NYI	GVT	TPP	NNN	VLV
SLC25A26	-SH	-NG	-IV	SLW	KYR	AES	GEQ	GGG	FIL	HQA	GGG	ILL	YF	AA	GGG	VYV	PKF	SSP	ATR	AVM
SLC25A38	LRT	KSL	VII	VYF	RHK	TSD	EEY	SGG	LHL	LRR	GGG	LLF	WFF	KSQ	GGG	MLG	STI	PAP	STR	ILA
SLC25A42	YIT	YRI	TIV	YSR	LRE	NEE	EEG	GGA	FLV	LKR	STG	LLL	WYY	RHK	GGG	NFL	SMS	APM	TNN	MVW
SLC25A46	YIN	SLT	FEI	NCR	KVQ	TKE	QEE	GGG	PIV	RGF	ARG	LVF	WII	Y	KGK	GMG	MGF	GVG	SPA	THV
Repeat 1	59	60	61	62	63	64	65	66	67	68	69	70	71	72	73	74	75	76	77	78
Repeat 2	162	163	164	165	166	167	168	169	170	171	172	173	174	175	176	177	178	179	180	181
Repeat 3	259	260	261	262	263	264	265	266	267	268	269	270	271	272	273	274	275	276	277	278

cytoplasmic gate

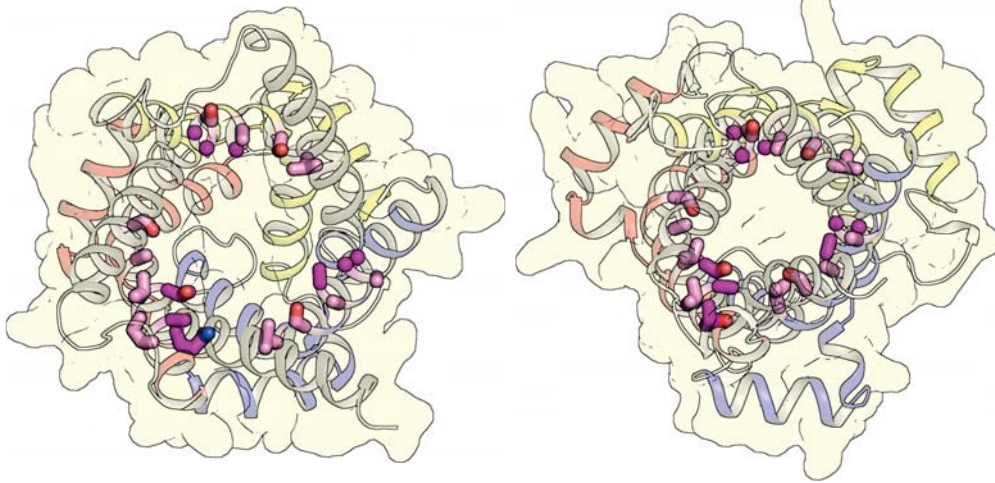
	substrate binding site	πxxxTπ aromatic motif	aromatic plug	tyrosine brace	cytoplasmic network															
	Φ	X	Φ	P	X	X	Π	Φ	ξ	Φ	Π	Φ	Y/F	E/D	ξ	Φ	K/R	ξ	Φ	
SLC25A01	YLG	GRM	SQV	IGC	PST	KND	AQV	AAA	VII	RVR	FFF	GFV	MVI	FMY	EED	FSE	LLV	SRV	NNK	HWL
SLC25A03	LMI	GRM	YQI	SIG	MPT	QYL	GTT	LMA	CML	KKQ	FFW	GAF	FCI	YFY	ETD	VRS	FTV	KVK	VEV	LAY
SLC25A04	IQL	GRM	YIG	FIM	PIG	TYG	QRA	AAF	LA-	NYV	FFL	AGV	FVL	KYY	DDD	KTE	YAI	KKK	QKQ	MY
SLC25A12	ILF	GRR	VDS	AIS	PPP	EFC	KSF	AAG	IIV	KYT	LFL	TPV	VVT	NYV	DAE	FHL	VCL	RKQ	DLR	KLW
SLC25A13	LLF	GRM	VDS	AIS	PPP	EFC	KSF	AAG	IIV	KYT	LFL	TPV	VVT	NYV	DAE	FHL	VCL	RKQ	DAR	KSW
SLC25A15	ILI	GRM	VDS	AIS	PPP	EFC	KSF	AAG	IIV	KYT	LFL	TPV	VVT	NYV	DAE	FHL	VCL	RKQ	DAR	KSW
SLC25A16	ILI	RGR	IMC	FAI	PPP	YYS	GAQ	AGA	IVV	QSA	FFF	MFT	ATT	FFY	EGE	HTL	YLM	KKK	TSQ	VLF
SLC25A19	ILI	LAK	SIA	IFA	GPL	YYS	GAT	AGG	VLV	QQM	FFF	LSF	SCS	FYY	ESE	MSF	LLF	TKC	EHN	LLV
SLC25A20	IMI	GRM	VDA	TVF	PPP	MAA	FSN	AGA	VMA	CYC	FFF	FML	GTG	FYF	GEE	LWV	GLA	KKM	KNK	LIF
SLC25A21	LGM	ARR	EHL	TGG	PVP	KFG	RNG	AMA	VVV	KYM	FFL	FGL	TfV	FYY	EYE	QNY	VYT	KKY	KNS	LMW
SLC25A22	TLL	LRV	VDI	TV	PPP	EFL	KSF	AVG	IIV	KYA	LFL	APV	ALV	NFY	DAF	FNL	FLG	RNI	HQA	QLE
SLC25A24	ILM	GRK	IIV	AII	PPP	EYA	TAV	AGG	VII	KDS	FLY	VAV	AVV	YYY	EEE	QLN	YLM	KKK	KSQ	LYT
SLC25A26	ILA	GRA	SEI	FIS	PPL	NFG	ASG	ALF	AVI	FQF	FFL	IPG	TLA	YWY	EED	YSR	VLT	KKH	WAS	FLL
SLC25A38	VLL	RGR	CDR	VAT	PPP	LGI	GFM	VSA	GGA	IIM	YVA	FLW	GMT	TFV	LYY	YNE	SQE	LTM	KKM	QNA
SLC25A42	VLV	RGK	VVG	VIP	PPP	PPI	YVA	AAV	AGG	ILL	QSS	FFF	SFT	ATT	HYF	EED	ETL	YLM	KKQ	RSI
SLC25A46	IKI	VRQ	QLY	GLT	VPL	TLH	LLA	GSA	ALV	EIL	GFQ	IPV	ITT	SVK	ELI	FHI	TGY	PVS	LLT	PHL
Repeat 1	79	80	81	82	83	84	85	86	87	88	89	90	91	92	93	94	95	96	97	98
Repeat 2	182	183	184	185	186	187	188	189	190	191	192	193	194	195	196	197	198	199	200	201
Repeat 3	279	280	281	282	283	284	285	286	-	287	2									



A

*cytoplasmic state*

*matrix state*



B

*cytoplasmic state*

*matrix state*

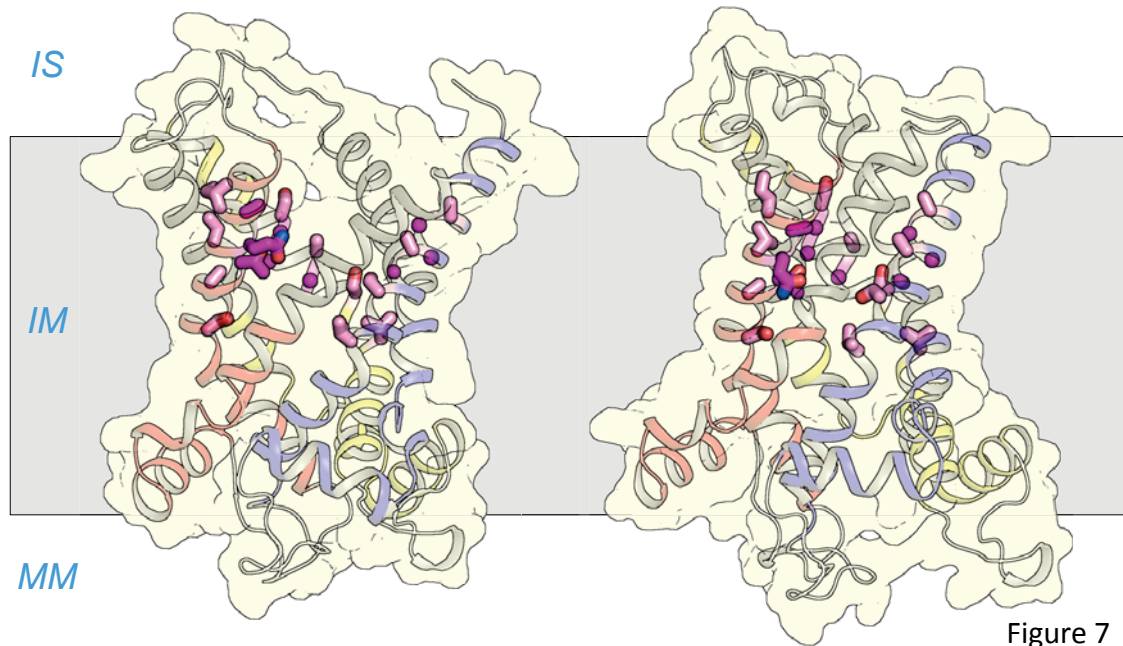
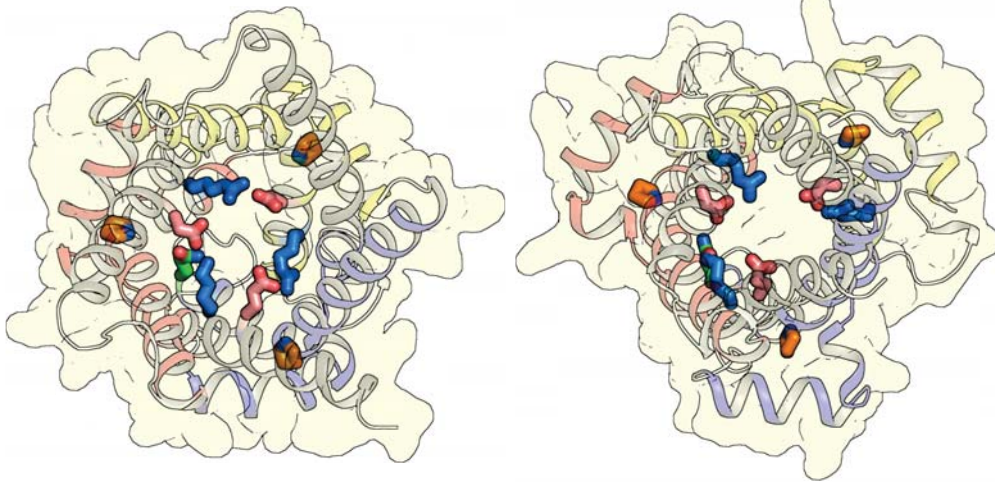


Figure 7

**A**

*cytoplasmic state*

*matrix state*



**B**

*cytoplasmic state*

*matrix state*

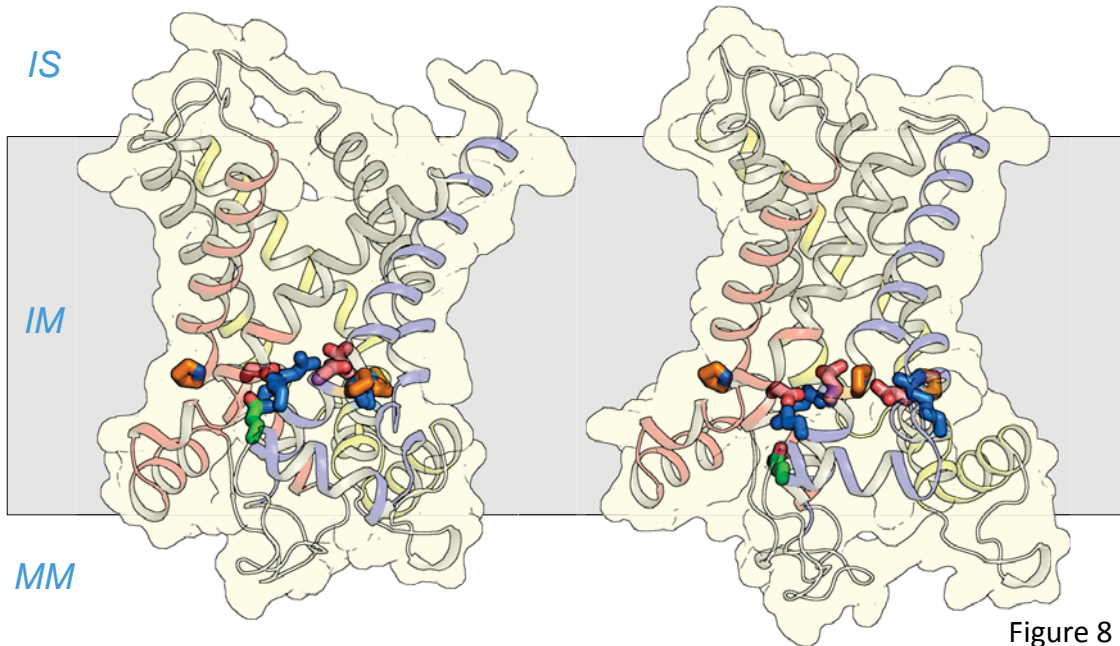


Figure 8

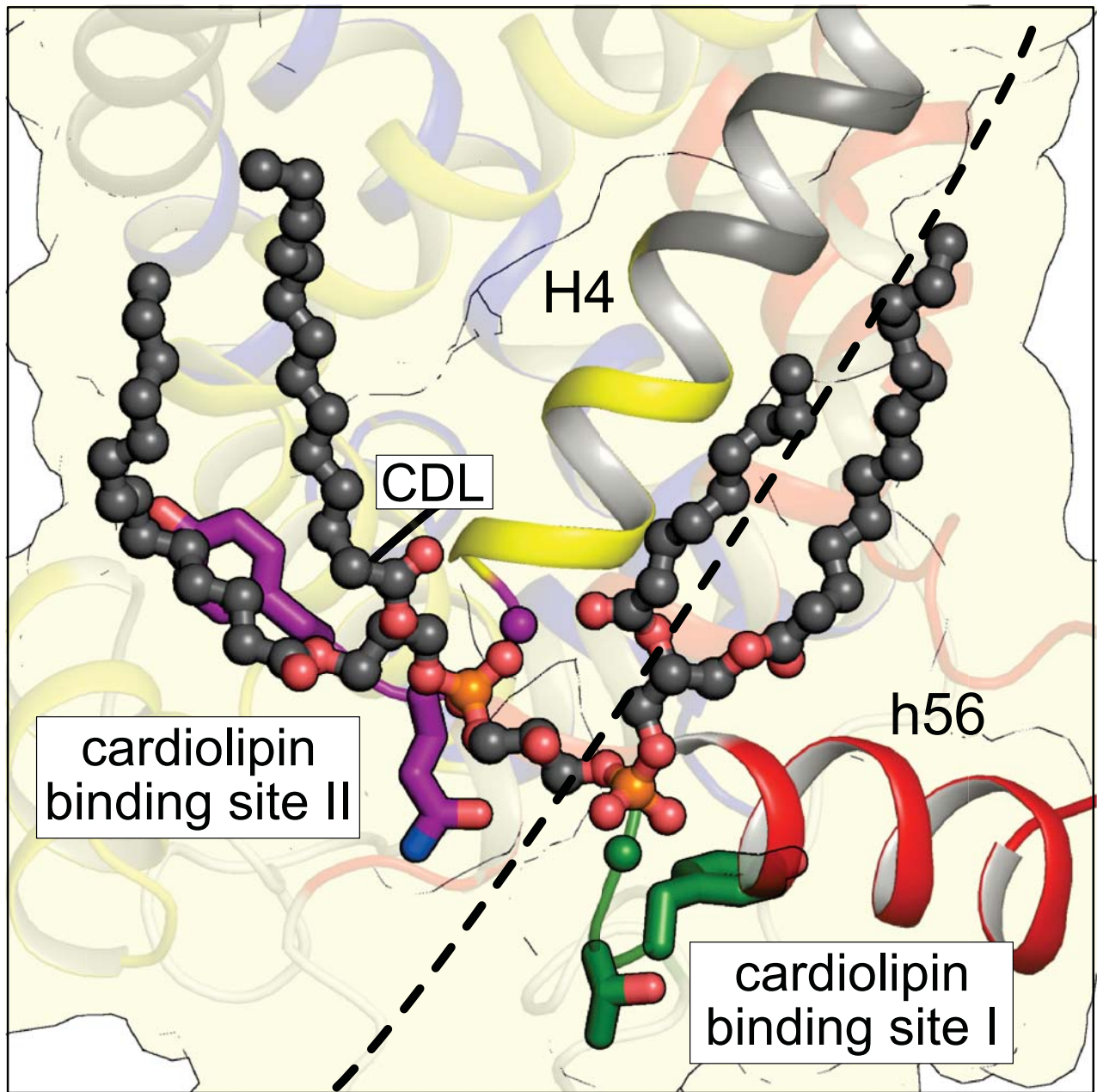


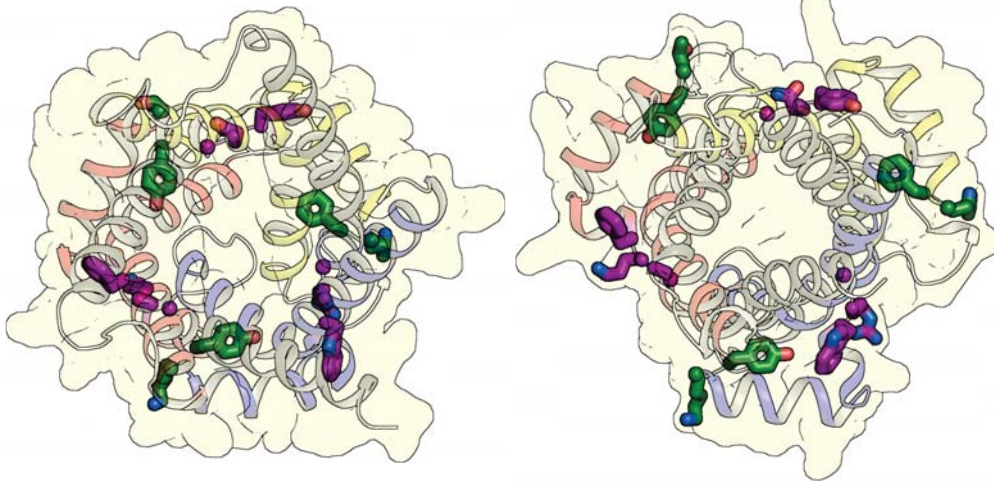
Figure 9



A

*cytoplasmic state*

*matrix state*



B

*cytoplasmic state*

*matrix state*

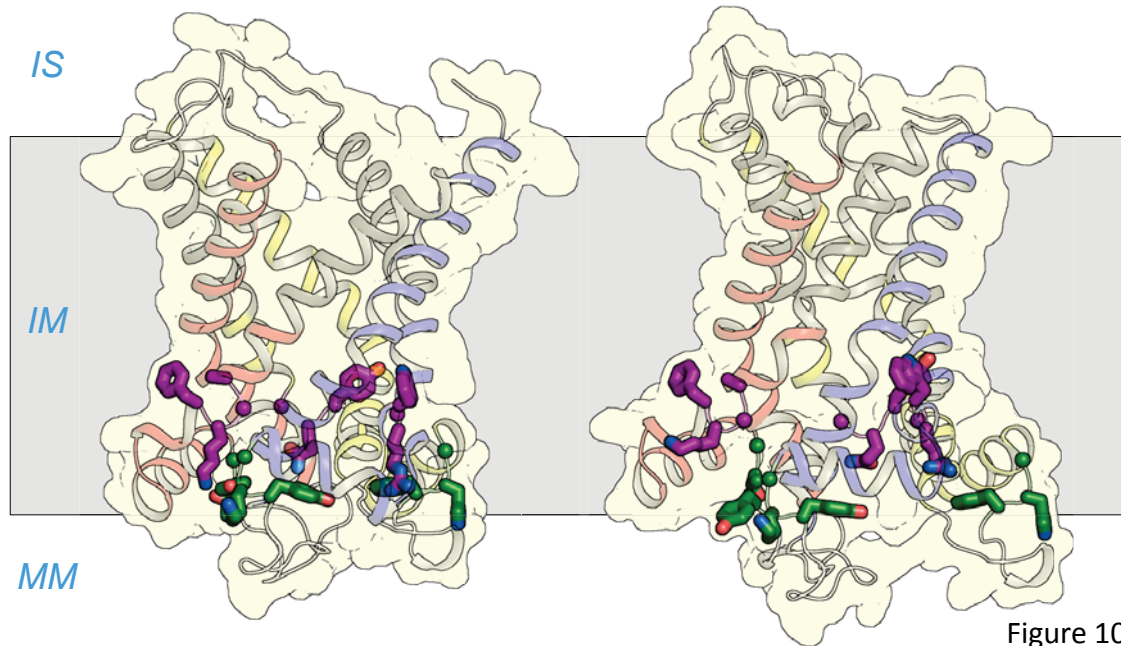


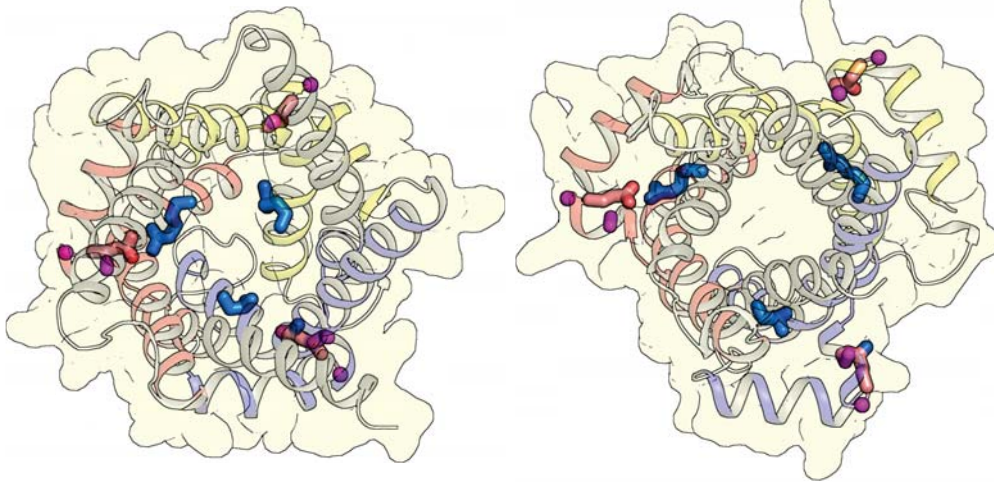
Figure 10



A

*cytoplasmic state*

*matrix state*



B

*cytoplasmic state*

*matrix state*

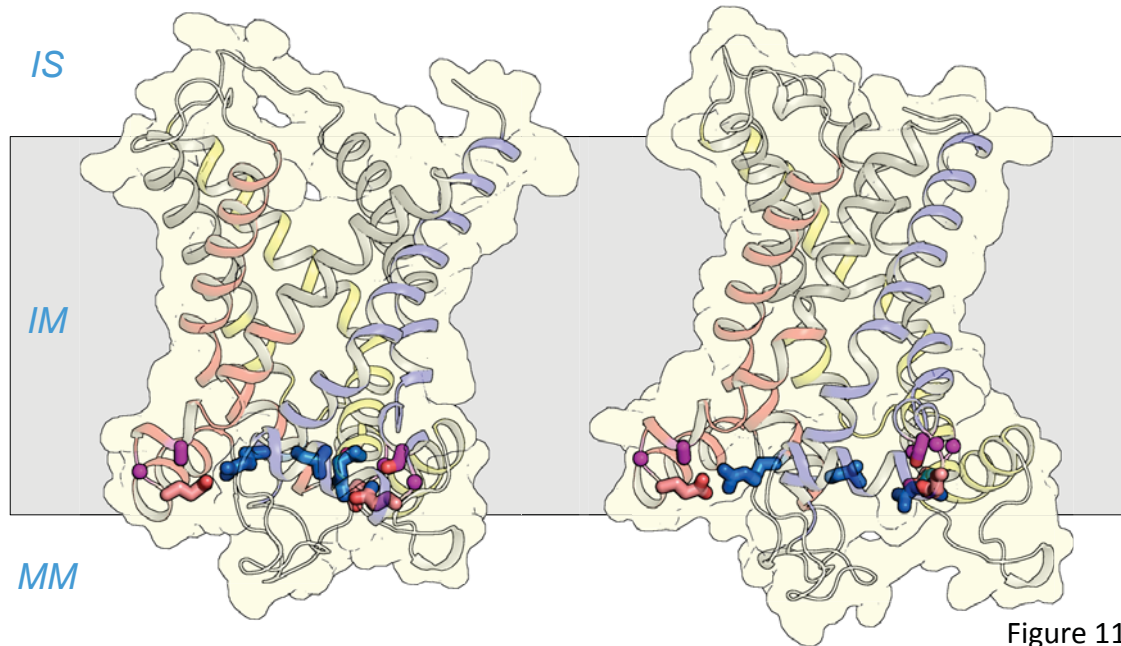
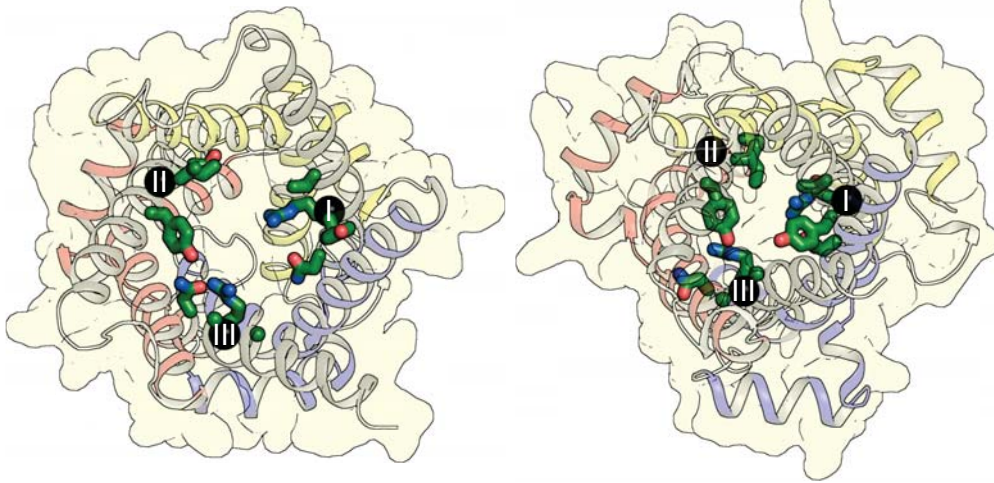


Figure 11

A

*cytoplasmic state*

*matrix state*



B

*cytoplasmic state*

*matrix state*

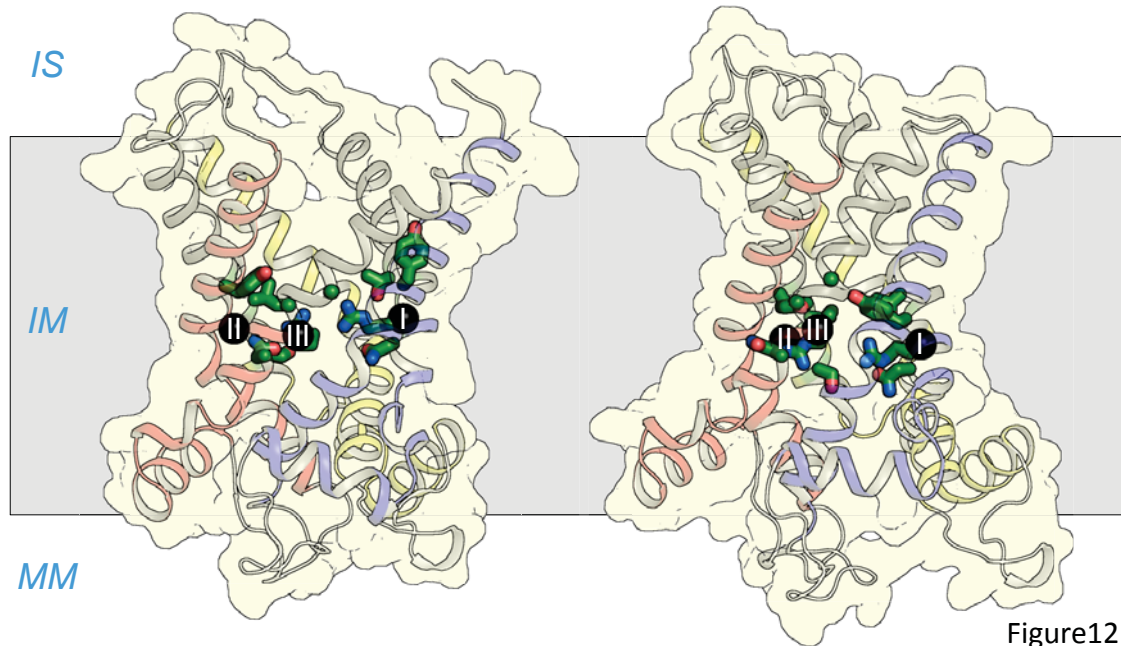
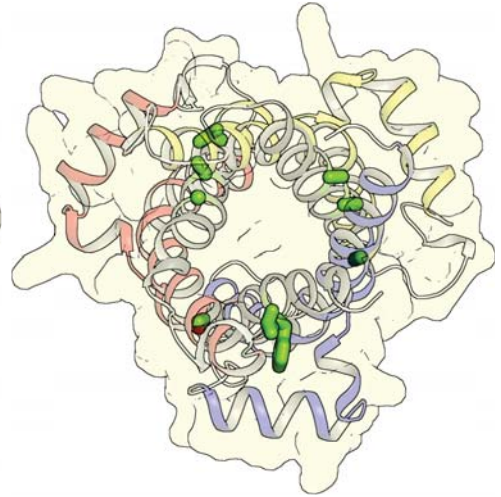
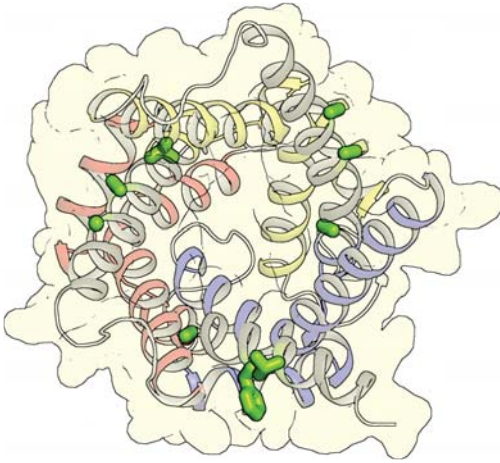


Figure12

A

*cytoplasmic state*

*matrix state*



B

*cytoplasmic state*

*matrix state*

*IS*

*IM*

*MM*

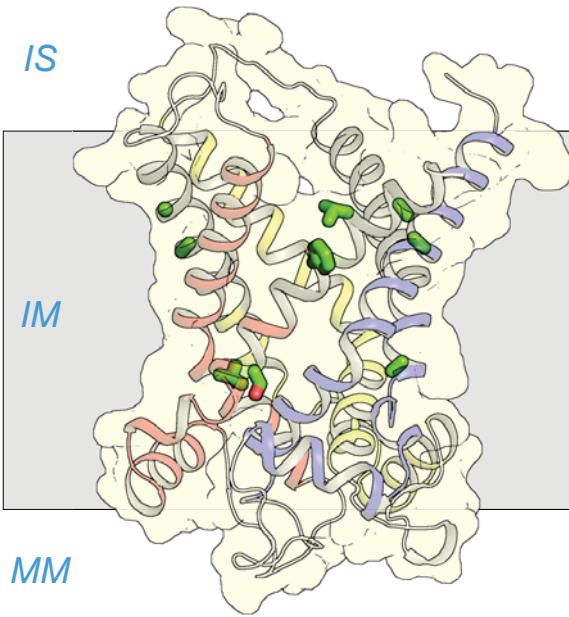


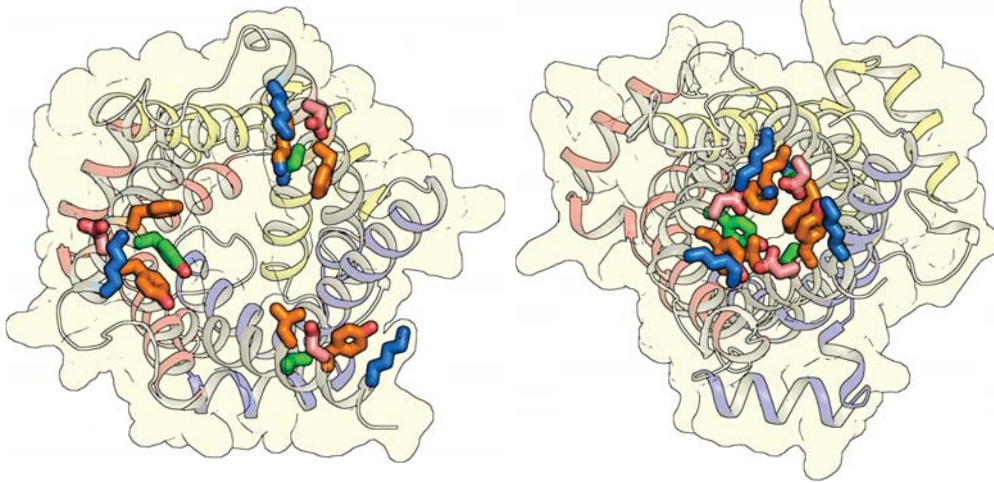
Figure 13



A

*cytoplasmic state*

*matrix state*



B

*cytoplasmic state*

*matrix state*

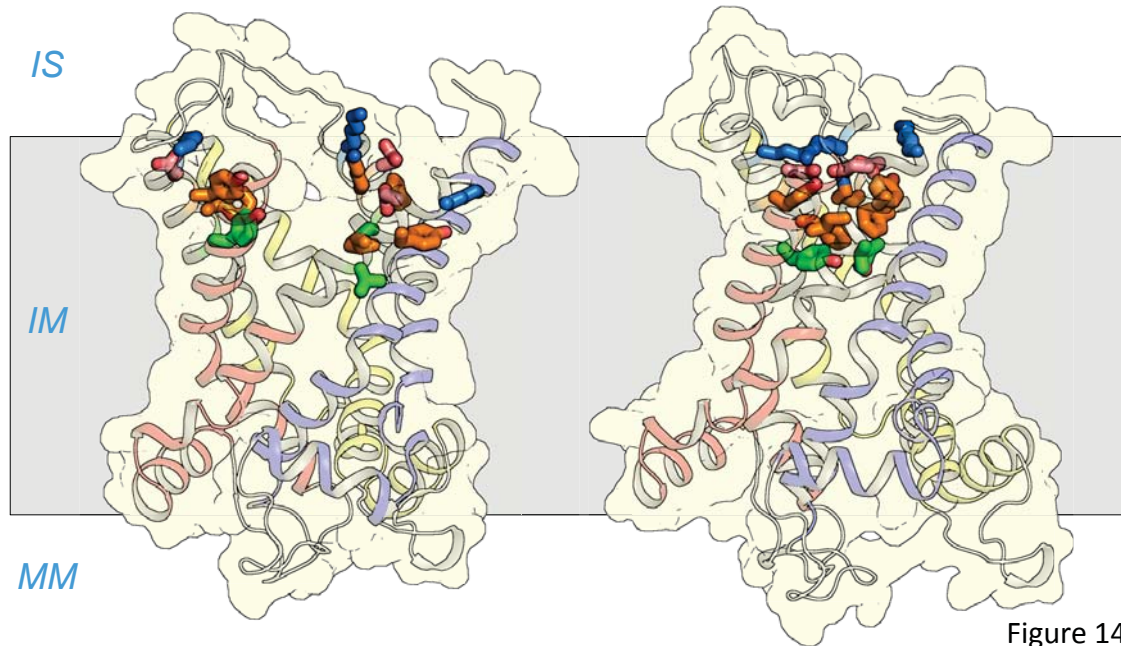


Figure 14